FU JEN STUDIES

NATURAL SCIENCES

NO. 24 1990

目 次 CONTENTS

續 (Continued)

Fu Jen Catholic University
Taipei, Taiwan, Republic of China

目 次（續） CONTENTS (Continued)

光纖去偏振調制對干涉訊號衰減效應之改善

柯　頓　黃仁芬

輔仁大學物理系

摘　要

本文係把調制式光纖去偏振器加接在光纖偏極型干涉儀輸入端，用以測試減輕信號衰減的效應。經過分析及實驗，發現當線性偏振輸入與去偏振器光纖主軸間夾角爲 0，$\pi/2$ 時，偏振態不穩造成的雜訊可降至最低，而輸入夾角爲 $\pi/4$ 時光源不穩造成訊號漂移亦可消除。

一、前　言

在光纖訊號輸出時，我們常會發現訊號有雜訊，甚至不穩定，可能是光纖受周圍環境影響使偏振態 (state of polarization 簡稱 SOP) 改變[1]，也可能是輸入光源本身不穩定所造成。

相干性高的光波，其偏振度 (degree of polarization) 也比較高，SOP 易受干擾而改變，我們可以用低相干性的光源或用去偏振技術來穩定輸出訊號，過去有人嘗試用各種不同方法來穩定輸出訊號[2~6]。本文以低雙折射光纖繞在PZT上，製成去偏振器，用在偏極型干涉儀之前，觀察干涉儀訊號輸出雜訊，以比較雜訊降低情形。

二、原　理

去偏振技術是使光波中的偏振光變成完全未偏振的光，對雷射光而言，它包含了偏振與未偏振的光，定義偏振度

$$P=\frac{I_{pol}}{I_{total}}, \qquad 0\leq P\leq 1$$

當 $P=1$，光爲完全偏振光。當 $P=0$，光爲完全未偏振光，光波的偏振均勻分佈在所有方向，且彼此之間相位獨立，毫無關連。

在本文中的去偏振器是將單模低雙折射光纖繞在圓柱型 PZT 上，使光纖產生對應快慢軸，（沿圓柱面法線方向之應力加在光纖上感生一慢軸，X；沿柱軸向——即垂直於法線向感生對應的快軸，Y）。

此時在 PZT 上加調制訊號，令其相位差 $\phi_X-\phi_Y=\phi_0+\Delta\phi_P \sin w_P t$，當調變頻率 $w_P \gg$ 檢測頻率時[7]

$$P=\left[1-\frac{4m^2(1-|J_0(\Delta\phi_P)|^2)}{(1+m^2)^2}\right]^{1/2}$$

此處 ϕ_0=相位差偏值。

$$\Delta\phi_P=2\pi k_0 nVNd_{33}\left\{1-\frac{n^2}{2}[P_{12}-(P_{11}+P_{12})\gamma]\right\}$$

k_0：光在眞空中的波數

n：光纖核心的折射率

V：加在 PZT 的作用電壓

N：光纖圈數

d_{33}：V 方向的 PZT 係數

γ：光纖的 Poisson 比值$=-\dfrac{\text{光纖橫向應變}}{\text{光纖軸向應變}}$

P_{11}：光纖同向光彈係數

P_{12}：光纖垂向光彈係數（卽應變與係數設定方向垂直）

$m=\tan\theta_i=\dfrac{E_Y}{E_X}$=入射 Y 軸向分電場與 X 軸向分電場比值

因此只要調整電壓令相幅 $\Delta\phi_P=2.4$，5.5，… 就可使 $J_0(\Delta\phi_P)=0$，以獲得 min P，完全去偏振光波則將發生在 $m=1$ 時。

圖 1 系統中光纖信號調相器與檢偏器（圖 1）實際代表一偏振型光纖干涉儀 (polarimetric interferometer)。上述去偏振調制器輸出的二分電場（沿 X，Y 二軸）再送接到此調相器上（二本徵軸爲 X' 及 Y'），它的調制相位差遂爲 $\phi_{X'}-\phi_{Y'}=\phi_0'+\Delta\phi_m \sin w_m t$，光波經此重新組合調相後，投射到偏振器軸向（與 X' 一軸夾成 θ' 角），構成二分電場的干涉輸出，由鎖相放大器檢取 w_m——基波訊號經計算遂爲

$$I_{w_m}=[(E_X^2-E_Y^2)J_1(\Delta\phi_m)\sin\phi_0'\sin 2\theta$$
$$+2E_XE_YJ_0(\Delta\phi_P)J_1(\Delta\phi_m)(\sin\phi_0\cos\phi_0'-\cos\phi_0\sin\phi_0'\cos 2\theta)]\sin 2\theta'$$

上式次項受去偏振作用影響，可調整 $\Delta\phi_P$ 以令 $J_0(\Delta\phi_P)\to 0$；另方面如無去偏調制，卽 $\Delta\phi_P=0$，則 $J_0(\Delta\phi_P)=1$。

訊號衰減設由二種來源所生，一爲光源擾動另爲輸入光偏振搖擺，

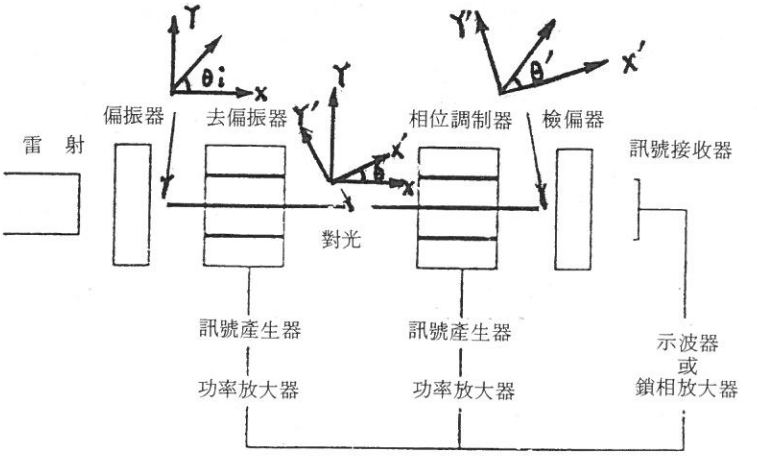

圖 1　測試訊號衰減裝置圖。

光源擾動可設：$E_X(t)=a_1n(t)$；$E_Y(t)=a_2n(t)$

$E_X^2(t)+E_Y^2(t)=a^2n^2(t)$ 爲時間函數

光偏搖擺可設：$E_X(t)=a\cos\theta_i(t)$；$E_Y(t)=a\sin\theta_i(t)$

$E_X^2(t)+E_Y^2(t)=a^2$ 爲常數

因此可比較其變率絕對值(即輸出穩定度) $\left|\frac{dI_{wm}}{dt}\right|$去偏，$J_0(\Delta\phi_P)=0$ 及 $\left|\frac{dI_{wm}}{dt}\right|$無去偏如表一所列。

三、實　　驗

訊號衰減 (singal fadings) 包含光強度不穩定和 SOP 擾動，而 SOP 擾動造成偏振衰減簡稱 P. F. (polarization fading)，依照上節之分析原理，本實驗採同一單模光纖內二偏振干涉 (polarimetric interference) 方式來做量測，在其前端加接一去偏振器 (scrambler) 以獲光波之低偏振度，遂可降低檢偏器訊號輸出之衰減效應，依此設計之裝置如圖 1 所示。

圖 1 中去偏振器和調制器加在偏振干涉光纖上分別以 A. C. 電壓調變，之後以示波器和鎖相放大器撿拾其輸出訊號。

表一 訊號衰減及去偏振調制改善效應分析比較

	$\theta_i=0$ 或 $\pi/2$ (a_2 或 $a_1=0$)	$\theta_i=\pi/4$ ($a_1=a_2=a/\sqrt{2}$)
未施加去偏調制	光源擾動時 $\left\|\frac{dI_{w_m}}{dt}\right\|=\|2a^2n(t)\dot{n}(t)\sin\phi_0'\sin 2\theta \cdot\sin 2\theta' J_1(\Delta\phi_m)\|$ 偏振向搖擺時 $\left\|\frac{dI_{w_m}}{dt}\right\|=\|2a^2\dot{\theta}_i(t)(\cos\phi_0\sin\phi_0'\cos 2\theta -\sin\phi_0\cos\phi_0')\sin 2\theta' \cdot J_1(\Delta\phi_m)\|$	光源擾動時 $\left\|\frac{dI_w}{dt}\right\|=\|2a^2n(t)\dot{n}(t)(\cos\phi_0\sin\phi_0' \cdot\cos 2\theta-\sin\phi_0\cos\phi_0') \cdot\sin 2\theta' J_1(\Delta\phi_m)\|$ 偏振向搖擺時 $\left\|\frac{dI_{w_m}}{dt}\right\|=\|2a^2\dot{\theta}_i(t)\sin\phi_0\cos\phi_0' \cdot\sin 2\theta' J_1(\Delta\phi_m)\|$
施加去偏調制	光源擾動時 $\left\|\frac{dI_{w_m}}{dI}\right\|=\|2a^2n(t)\dot{n}(t)\sin\phi_0'\sin 2\theta \cdot\sin 2\theta' J_1(\Delta\phi_m)\|$ 偏振向搖擺時 $\left\|\frac{dI_{w_m}}{dt}\right\|=0$ 顯著改善偏振訊號之衰減效應	光源擾動時 $\left\|\frac{dI_{w_m}}{dt}\right\|=0$ 顯著改善光源擾動（但輸出之 I_{w_m} 變小，可能不易檢測） 偏振向搖擺時 $\left\|\frac{dI_{w_m}}{dt}\right\|=\|2a^2\theta_i(t)\sin\phi_0'\sin 2\theta \cdot\sin 2\theta' J_1(\Delta\phi_m)\|$

實驗光源採用波長 0.63 μm 散亂偏振的 He-Ne 雷射，經偏振器產生線性偏振光波送進單模光纖，經去偏振器產生相位調變，讓偏振度降低，再將光通過調制器作相位調變（即相當於訊號加入），經偏振器後兩模態的光互相干涉輸出。

本實驗所用的去偏振器調制頻率爲 45KHz，調制器的調制頻率則爲 23KHz，在輸出端以 PSD (phase senstive detector) 將輸出訊號經鎖相放大器（即以調制器的調變頻率爲參考頻率）取出所要的信號。

經過鎖相放大器的輸出信號，可直接由鎖相放大器接示波器或由 X-Y recorder 看出整個訊號的擾動過程。

圖 2 爲未去偏振前的訊號，加上去偏振以後如圖 3，去偏振電壓=7.8 vlots，$\theta_i=0$。比較圖 2 和圖 3，去偏振後輸出訊號較近於水平。由上節理論分析（表一）得知本實驗原有訊號衰變係由入射偏振向搖擺所致。

圖 4（未去偏振）及圖 5（去偏振後）中 $\theta_i=\pi/4$，去偏振電壓=7.0 vlots。由同一於圖二及三之偏振向搖擺所導致的訊號衰變去除效果較差，此跟表一分析者相一致。

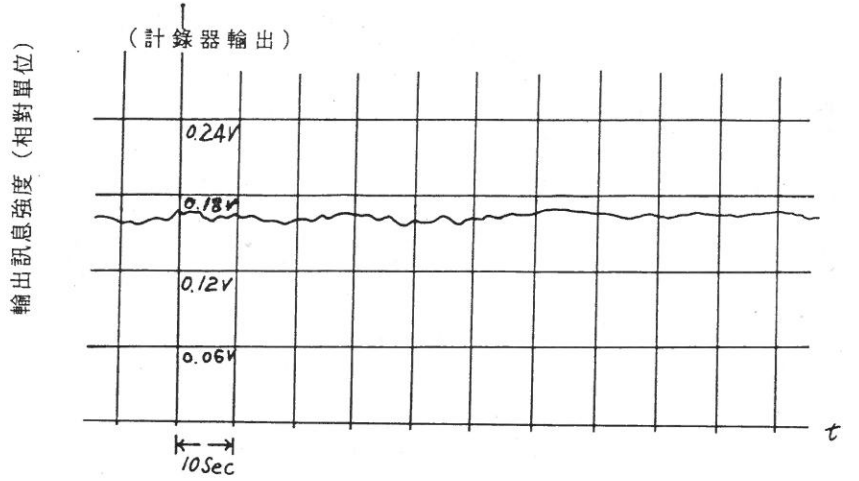

圖 2 未加去偏振調制的訊號衰變檢測 ($\theta_i = 0°$)。

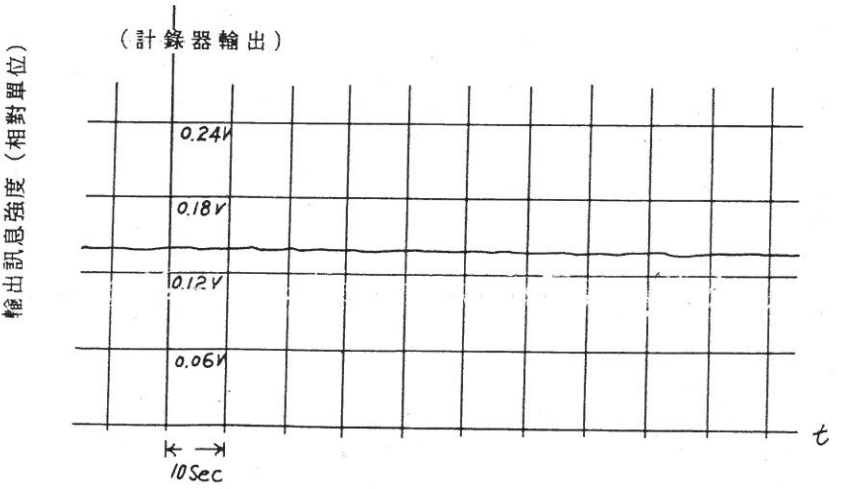

圖 3 施加去偏振調制（對應於圖 2）改善訊號衰變檢測效應 ($\theta_i = 0°$)。

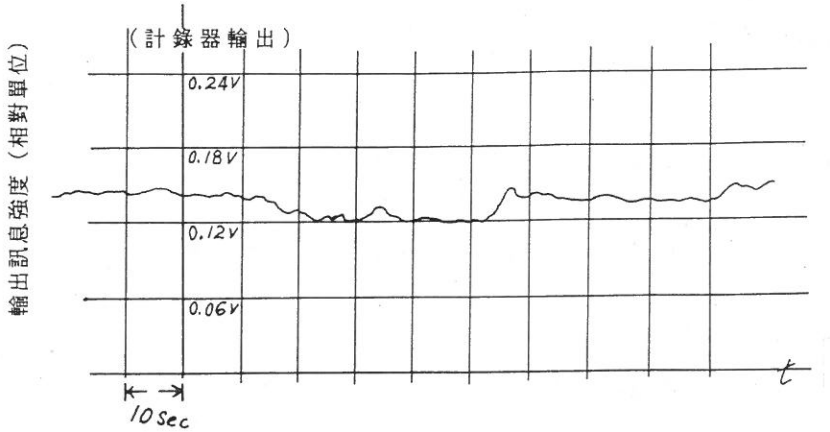

圖 4 未加去偏振調制的訊號衰變檢測（$\theta_i=\pi/4$）。

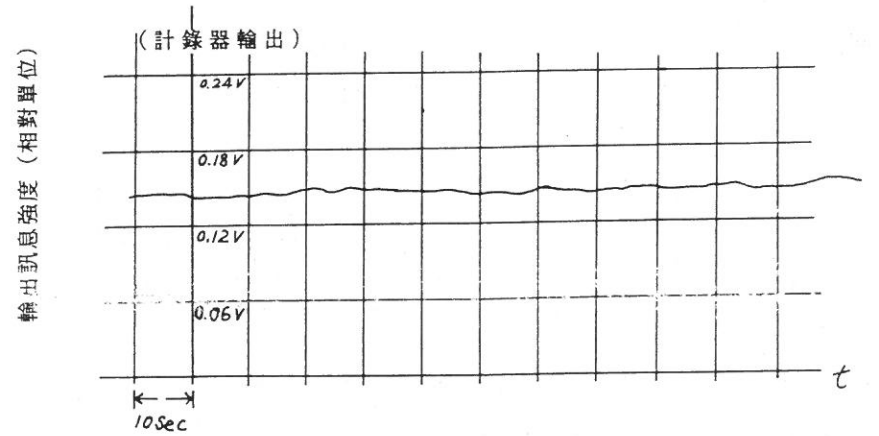

圖 5 施加去偏振調制（對應於圖 4）訊號衰變改善效應（$\theta_i=\pi/4$）。

四、結　　論

利用光纖纏繞 PZT 製成相位調制去偏振器，若加在 "one arm" 光纖偏極型相位干涉儀之前，能降低訊號干擾現象。以線性偏振光輸入，相對主軸夾角爲 0 或 $\pi/2$ 能消除偏振軸擾動現象，夾角等於 $\pi/4$ 時光源不穩的影響可被除去。

參 考 文 獻

(1) D.W. Stowe, D.R. Moore and R.G. Priest, "Polarization Fading in Fiber Interferometric Sensors", *J. Quantum Electron.*, **QE-18**, 1644 (1982).
(2) B. Hillerich and E. Widel, "Polarization Noise in Singal Mode Fibres and Its Reductihn by Depolarizers", *Optical and Quantum Electronics*, **15**, 281 (1983).
(3) N.J. Frigo, A. Danaridge and A.B. Tveeten, "Technique for Elimination of Polarization Fading in Fibre Interferometers", *Electronics Letters*, **20**(8), 319 (1984).
(4) P. Granestrand and L. Thylen, "Active Stabilization of Polarization on a Single-Mode Fibre", *Electronics Letters*, **20**(9), 365 (1984).
(5) A.D. Kersey and A. Dandridge, "Monomode Fibre Polarisation Scrambler", *Electronics Letters*, **23**(12), 634 (1987).
(6) A.D. Kersey, A. Dandridge and A.B. Tveten, "Elimination of Polarization Induced Singal Fading in Interferometric Fiber Sensors Using Input Polarization Control", *OFS*, p. 44 (1988).
(7) P. Ramon, De Paula and Emery L. Moore, "Review of All-Fiber Phase and Polarization Modulators", *SPIE*, Fiber Optic and Laser Sensors II, **478**, 3 (1984).

Improving the Signal Fading of the Fiber Interferometer with the Fiber Depolarized Modulation

TON KO AND JAN-FAN HWANG
Fu-Jen University, Physics

ABSTRACT

A Single-mode fiber polarization modulator was empolyed at the input end of an interferometer to reduce the signal fading. The results showed the optimal angles between the direction of polarization of the linearly polarized input light and the optic axis of the fiber polarization modulator were 0 or $\pi/2$ for reducing polarization fading and $\pi/4$ for suppressing intensity fluctuations.

A STUDY OF THE POWER SPECTRA OF SUMMER TIME AMPLITUDE SCINTILLATIONS IN TAIWAN

JOHN R. KOSTER AND HSI-SHU WU

Department of Physics
Fu Jen University

ABSTRACT

Continuous recordings of the night time scintillations of 136 MHz radio waves were made at the ionospheric physics lab of Fu Jen University over the period June 13-July 6, 1990. The S4 parameter was determined and power spectra produced for 636 of these records. A novel method of classifying power spectra is developed and used. A study of occurrence times, S4 values, asymptotic slopes and the characteristics of the power spectra lead to the conclusion that only a small fraction of the Taiwan night time scintillations during summer can be accounted for by the equatorial bubble (EB) mechanism. The remainder must arise from a different physical mechanism, the nature of which is still to be determined.

1. INTRODUCTION

(1) Scintillations

Occasionally the radio waves received from an earth satellite or a radio star exhibit scintillations, i.e., rapid variations in amplitude. Scintillations are known to be produced by irregularities in the electron distribution in the E and F regions of the ionosphere. They are very frequent and severe near the dip equator, where the earth's magnetic field is horizontal—conditions favorable to the production of electron density depletions through the so-called Rayleigh-Taylor mechanism. This type of plasma instability, frequently referred to as an "equatorial bubble", has been extensively studied, and the physics involved is quite well understood. We shall refer to scintillations caused by these depletions as Equatorial Bubble (EB) scintillations.

Scintillations also occur at middle latitudes. These are usually less severe. The physical mechanism giving rise to them is not known. We shall refer to scintillations of this type as Mid-Latitude (ML) scintillations.

The work reported on here has been done with a view to ascertaining what mechanism is responsible for the amplitude scintillations observed on a 136 MHz radio wave in Taiwan.

(2) Scintillations in Taiwan

Scintillations in Taiwan have been studied by a number of workers, especially by Huang[1,2]. He has shown beyond reasonable doubt that much of the scintillation observed in Taiwan, especially during the equinoctial seasons, is of the EB type. There is little scintillation activity during the winter months in Taiwan, but scintillations, especially smaller ones, are extremely frequent around the time of the June solstice, a season when the bubble mechanism is known to have a minimum of activity. This paper addresses the question of the origin of these summer-solstice amplitude variations observed in Taiwan.

(3) The Characteristics of EB type scintillations

Equatorial Bubble type scintillations can usually be identified in the chart records of the amplitude of the radio signal received. The characteristics are:

(a) The scintillation rate is high—typically 1 to 10 Hertz.

(b) The onset of the scintillations is abrupt. The record changes from no scintillations to severe amplitude variations within a few minutes.

(c) The cessation is usually abrupt, also. But it does at times exhibit a slow diminution to zero in both amplitude and rate of the scintillations.

(d) The value of the d.c. component of the signal is somewhat reduced—the scintillations rise above and below a level somewhat below that of the pre-scintillation record.

It is sometimes difficult to classify a particular period of scintillation with certainty.

2. THE MEASUREMENT OF SCINTILLATIONS

(1) The S4 parameter

One of the widely used measures of the severity of amplitude scintillations is the S4 parameter. This is defined as the normalized second moment of intensity. Since 'intensity' involves the square of the amplitude, its second moment involves the 4th power of the amplitude of our received radio signal—hence the 4 in its name. The details of its determination need not concern it here. We merely note that it is done in a routine way with the aid of a very simple computer subroutine. Values of S4 are normally in the range 0 to 1, with 0 indicating no scintillations and 1 indicating severe amplitude fluctuations. In practice, in this paper, S4 values less than 0.1 will not used—they are too small to analyze with accuracy. Values above 0.5 are considered large scintillations. Values above 0.8 are 'saturated'—so large that the S4 value has little numerical significance beyond the fact that the scintillations are too severe to be determined with accuracy at the frequency being used.

(2) Power spectra

The power spectrum, giving the frequency of the amplitude variations as well as the amplitude at each frequency, is a powerful tool in the analysis of scintillations. Koster and Peng Wang[3] have shown that the production of good quality power spectra is possible using radio signals from the satellite source ETS-2. There is a problem because of the existence of some spectral lines due to the spin of the satellite. At times of high scintillation levels, these can be ignored, since their effect is negligible. At times of smaller scintillations, the interfering components may become a significant part of the total energy involved, and it becomes necessary to remove them before final analysis. Their presence makes it difficult to analyze extremely small levels of scintillation with accuracy.

The power spectra described here have been produced using the maximum entropy method. This method is somewhat faster than the standard Fast Fourier Transform procedures. The two types of analysis have been carefully compared, however, and the agreement is excellent. Spectra are normally presented with the log of the spectral estimate (energy per unit bandwidth) plotted as a function of the log of the frequency.

(3) A Classification scheme for power spectra

We are faced with the task of comparing a large number of individual power spectra. Some general classification scheme is needed to enable us to do this clearly and efficiently. A glance at a typical log-log power spectrum suggests the basis for a novel method of doing this. The shape almost invariably approximates very closely that of an inverted hyperbolic tangent, the equation of which can be written in the form:

$$Y=Y_0+A\tanh(B(X-X_0))$$

The four parameters have the following simple interpretation:

X_0, Y_0 are the coordinates of the center of symmetry of the hyperbolic tangent;
A is the amplitude of the hyperbolic tangent; and
B defines the slope of a hyperbolic tangent of unit amplitude.

The slope of the spectrum at its steepest point (the center of symmetry) is given by:

$$\text{SLOPE}=B\times A$$

Fitting a hyperbolic tangent to the experimental points of a given spectrum is an interesting exercise. In this analysis a function was devised which summed the absolute value of the distance between each experimental point and the smooth curve. A standard minimization routine was then used to find the minimum of the function. The method is conceptually simple, but consumes a great deal of computer time.

(4) Data base used

Fast data recordings were made during a 9-hour period on a continuous basis on 21 nights between 13 June and 6 July, 1990. Data were stored in files of 8,192 points each—the sampling rate being kept at 24 readings per second. Each file was subsequently investigated. If its S4 value exceeded 0.1, the file was retained for later analysis.

Not all such files were analysed, but a sample of 318 was chosen for full analysis. Since each of these yielded two power spectra (we used 4,096 points for each) we have a total of 636 power spectra—the data base for this study.

In the course of this three week period there were three large bubble "events"—periods of obvious bubble type scintillations. 92 of the 107 spectra with S4 greater than 0.5 fell on these three nights. The remaining 529 spectra represented modest scintillation levels, with no indications of the bubble mechanism being at work.

3. RESULTS

In this section we wish to look at results of the analysis of the 636 night time records of summer scintillation at Fu Jen University. We will look at the S4 values, the times of occurrence, the values of the center of symmetry of the spectra and the asymptotic slopes.

(1) The Distribution of S4 values

Figure 2 shows a histogram of the distribution of S4 values for the 535 cases where its value exceeded 0.1. There were, in addition, 101 cases where the S4 value fell below 0.1. These arose since files were chosen on the basis of the total S4 being >0.1. But in the analysis, where each file produced two spectra, it sometimes happened that the S4 for one of the half-files was below 0.1. These latter are not shown in the histogram, since their number is not a fair estimate of the total number of data sets with S4 <0.1. The actual number is surely much higher since, as the histogram shows, summer scintillation at Fu Jen is predominantly of the small S4 type. It is difficult to get an accurate appraisal of the S4 values at very low levels, however,

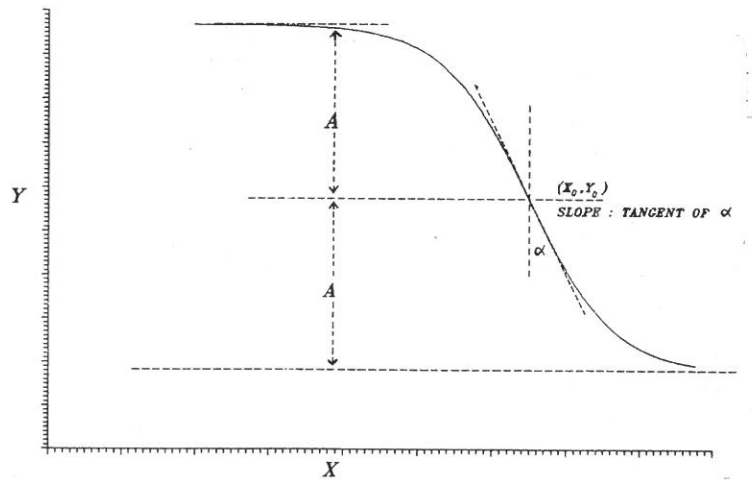

Fig. 1. The parameters of a hyperbolic tangent as fitted to a log-log power spectrum.

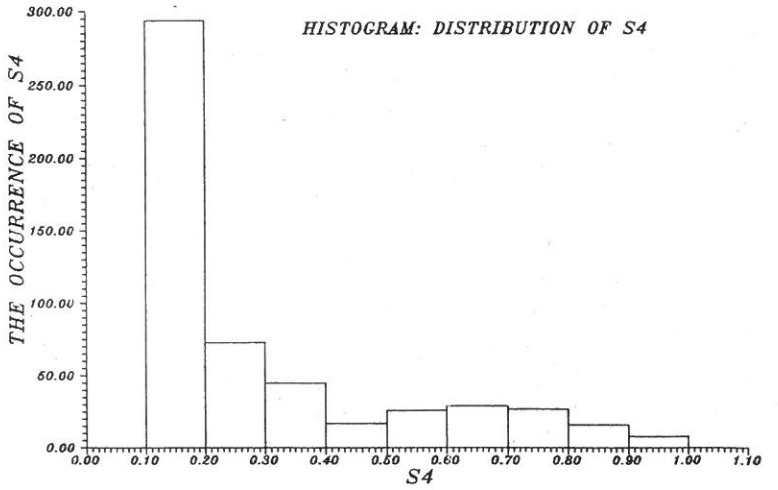

Fig. 2. Histogram of the occurrence of various S4 levels.

since the spurious spectral lines introduced by the satellite spin mentioned above produce an S4 value of 0.055 in our records, even when there is no scintillation at all. Over 80% of the scintillation records included in this study have S4 values <0.5. This percentage must be taken as a lower limit; the actual value is almost certainly higher.

(2) The distribution of scintillations with time of night

Figure 3 shows the distribution of occurrence times by hour for the 636 spectra examined. It should be noted that, as an aid to analysis, a night is specified by the date at sunset. Hours then run continuously from 18 to 32, the date remaining unchanged. The most probable time is seen to be 26 hours (2:00 a. m.).

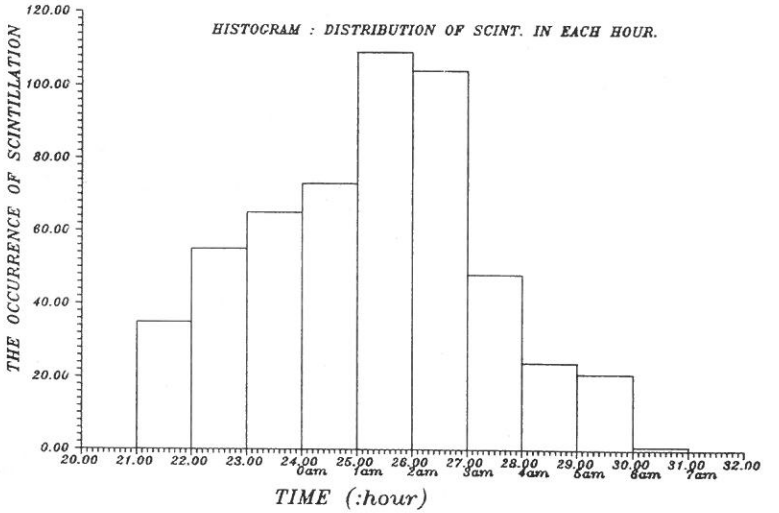

Fig. 3. Histogram of the distribution of cases of scintillation as a function of local time.

Figure 4 shows a corresponding plot of the time distribution of scintillations with S4 $>$0.5. Attention is called to the fact that the peak in this distribution falls an hour or more before midnight—a well known characteristic of equatorial bubbles. The above difference in distributions is considered to be significant.

(3) Distribution of the centers of symmetry of the spectra

It is interesting to study the variation of the X_0, Y_0 values during a typical ionospheric bubble type of event. We show this in Fig. 5, where we plot the location of the center of symmetry for the first 15 spectra obtained on 21 June, 1990. The spectra begin at 22:00 local

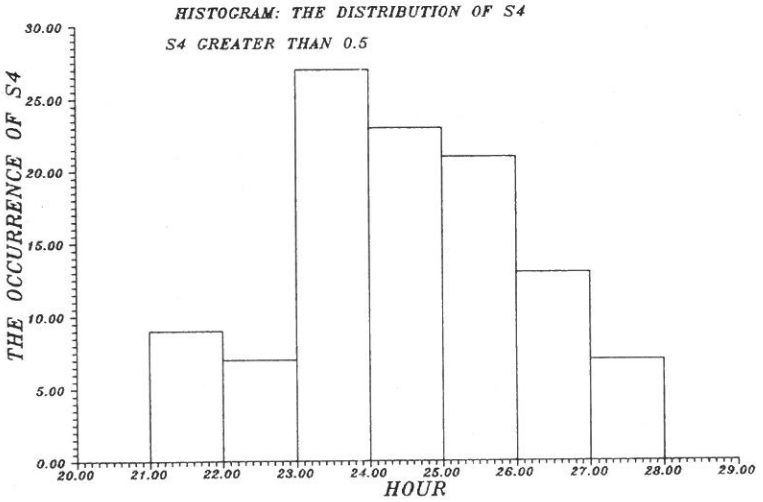

Fig. 4. Histogram of the distribution of cases of scintillation with S4>0.5.

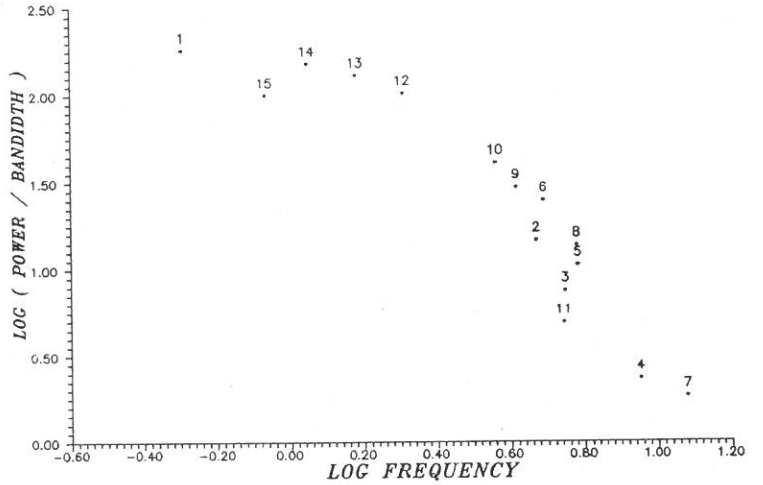

Fig. 5. The variation of X_0, Y_0 (the center of symmetry) of the spectrum with time during a typical bubble event.

time, and cover 43 minutes of time. Each point in the graph has been given its respective number in the 15-spectrum sequence, so that the movement of the center of symmetry with time can be easily followed.

If one were to join the points in chronological order, the movement would be a rapid clockwise motion at the very beginning, followed by a slow and predominantly anti-clockwise movement back towards the starting point. This variation with time is a characteristic of bubble events, and will be commented on later. It should be noted that the points lie roughly on the arc of a quarter circle, centered in the origin. None of the points fall in the central region of the quarter circle.

Most of the spectra (428) described here were taken on days when there was no evidence of the occurrence of an ionospheric bubble any time during the night. The location of the centers of symmetry of these appear as asterisks in Fig. 6. The location of the center of symmetry during bubble type events (198 spectra in all) are shown as squares in the same figure. A number of spectra occurring on bubble days but not directly associated with the bubbles are omitted from the plot.

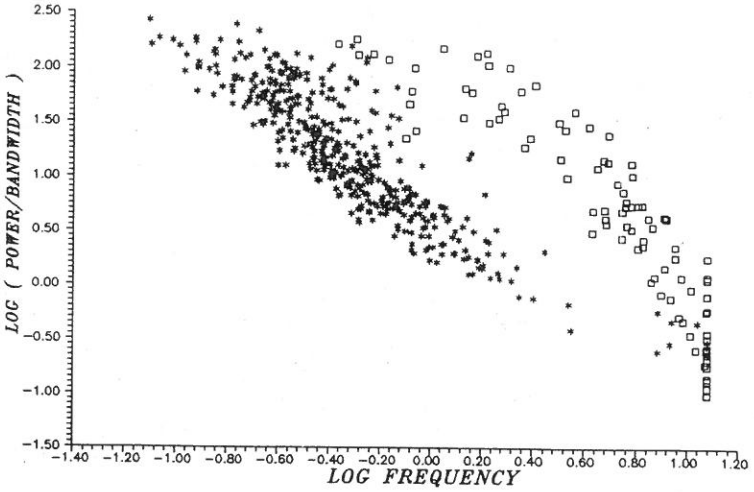

Fig. 6. A mass plot of the X_0, Y_0 values for spectra taken curing bubble events (squares) and for cases of ML scintillations (asterisks).

(4) The Distribution of the asymptotic slopes of the spectra

Figure 7 is a scatter plot of the value of the asymptotic slope $(B \times A)$ for each of the spectra as a function of the S4 value of the

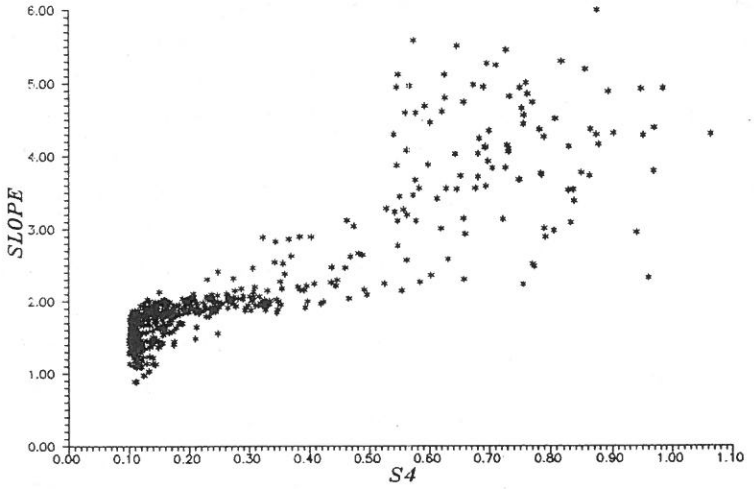

Fig. 7. Mass plot of the value of the asymptotic slope of the power spectra as a function of their S4 value.

scintillation which was used to produce the spectrum. It will be recalled that a spectral slope of the order of 2 is associated with a single scattering mechanism; significantly higher slopes are indicative of a multiple scattering mechanism.

4. DISCUSSION

Some discussion of the significance of the center of symmetry of our spectra and its movement with time is called for, since this is a rather novel method of classifying spectra. The center of symmetry itself lends itself to a rather simple physical interpretation.

X_0 is the log of the frequency at which the power density (measured in db) falls to 1/2 its maximum value.

Y_0 is a measure of the power density (db) at the mid range frequency component of the spectrum. It is also half the amplitude of the power density at the low frequency end of the spectrum.

A simple interpretation of the variation of X_0, Y_0 with time during the course of a bubble event could be roughly this:

(a) Early in the lifetime of the bubble, the frequency components of the spectrum cover a broad range (X_0 is large) and the ratio of the amplitude at low frequencies to that at mid frequency range is modest (Y_0 is small). This may be due to the fact that only a fraction of the energy from the satellite is scattered in the forward direction.

(b) As time proceeds, the smallest irregularities (the highest frequencies) disappear first, follower later by the larger ones. More of the total energy is now scattered in the forward direction, and the value of Y_0 rises as X_0 decreases.

(c) The process proceeds until (as usually happens) the scintillation abruptly halts as the eastward ionospheric drift carries the westward edge of the bubble beyond our line of sight. Alternatively, the amplitude and frequency of the scintillations may slowly die out, due both to a decrease in the ionospheric drift velocity and the disappearance of the irregularities as a result of ionospheric recombination processes. In this case, the center of symmetry moves into the central portion of the quarter circle.

5. SUMMARY AND CONCLUSIONS

A comparative study has been made of EB and ML types of scintillation found in the records made at the ionospheric physics laboratory at Fu Jen University. The main findings are:

(a) ML and EB types of scintillation have a different distribution of probability of occurrence with time of night. ML scintillations exhibit a peak around 2:00 local time. The EB scintillations have a peak around 23:00 local time.

(b) ML and EB scintillation types have different S4 values. S4 for ML type scintillations is generally in the range 0.1 to 0.5. The S4 values for EB scintillations are typically in the range 0.6 to 0.8 or even higher.

(c) The spectra of ML and EB types of scintillation have different asymptotic slopes. ML scintillations have spectral slopes in the range 1.5-2.5; values typical for a single scattering mechanism. The slopes for EB type scintillations are of the order of 5.0; values associated with a multiple scattering mechanism.

(d) The centers of symmetry of the two types of spectra not only fall at different places on the log-log plot; EB spectra also display a systematic variation with time not found in the case of the ML spectra.

(e) ML scintillations have a large occurrence peak at the June solstice; EB type scintillations have an occurrence minimum during that season.

Our conclusion is that the assumption that the two types of scintillation have their origin in a common physical mechanism is untenable. The mechanism which produces EB scintillations is well known. The mechanism responsible for ML scintillations is still not known. We hope to help find it.

REFERENCES

(1) Y.N. Huang, *J. Geophys. Res.*, **90**, 4333 (1985).
(2) Y.N. Huang, *J. Geophys. Res.*, **95**, 4297 (1990).
(3) J.R. Koster and E.P. Wang, *Fu Jen Studies*, **23**, 1 (1989).

臺灣夏季閃爍現象之光譜研究

高 士 達　　吳錫樹

輔仁大學物理系

摘　　要

於 1990 年 6 月 13 日至 7 月 6 日期間在輔大電離層實驗室用 136 MHz 的無線電波在晚間作閃爍值測量。此測量共有 636 個紀錄用來決定 S4 參數值及作光譜圖分析。規劃光譜圖所用的方法是新的，可以用來決定光譜圖中 S4 值的取樣點。

從閃爍現象出現的次數，S4 值，趨近斜率值，及光譜圖的特徵可以得到推論——在夏季閃爍所造成的原因，只有一小部份是由「汽泡型」機制所造成的，而造成主要閃爍原因的不同機制尚在研究之中。

餐飲管理之電腦輔助教學系統

全 中 妤

輔仁大學生活應用科學系餐飲管理組

摘　　要

爲了將複雜的餐飲業務組織工作提升至電腦管理的境界，吾人已結合餐飲管理的概念與電腦的科技，發展出一套教學系統做爲工具。原設計目的本在使系上同學應用電腦擴大管理層面，但正視整套軟體，相信亦有助於各醫院學校的餐飲管理工作。

本系統計分四大子系統，詳細名稱及功能如下：

一、庫存採購系統：食物種類及採購規格，現今庫存及建議採購量，採購單與撥發單的印製，單日採購／撥發報表，本月採購／撥發報表。

二、食物製備系統：食譜名單，標準食譜制定，菜單選擇，調整食譜，預製名單，材料需求名單。

三、食物成本系統：食譜成本計算，製備成本報表，每日食物成本報表，本月食物成本報表，本月盤存及單物成本總報表。

四、飲食評估及營養分析系統：食物營養成份表，食譜營養分析，個人身體記錄及營養建議量，個人每日飲食營養評估。

爲方便國人學習與使用，本系統採用個人電腦及中文系統來制定。目前已開發完成並已獲得內政部著作權執照，期望其功能能從學校擴展至業界，且對實質的餐飲管理工作有所貢獻。

一、前　　言

一般的餐飲週期 (Foodservice cycle)；如圖 1，可分爲三期：銷售期前 (presale phase)，銷售期間 (point-of-sale phase) 和銷售期後 (post-sale phase)；主要的產物就是食物和服務。銷售期前主要爲預製的工作，即將食物材料買進驗收儲存，撥發清洗預製和估價定餐，這些工作均是在交易形成之前所必需準備妥當的。當客人點菜，服務生捧出佳餚後，交易就開始成立，工作還包括服務，付帳等。在銷售期後多半做內部的檢討工作，包括帳務管理，菜單設計，分析等工作。整個期間可以說是將資源轉換爲產品，把客人放置在一個被服務的環境中，以求換得相當的金錢或代價做爲報酬，而所得到的成果無論是好是壞，實際的記錄均有助管理者再改進再突破，以求事業的生存與發展。

縱觀整個餐飲管理的工作實在是十分的複雜，其中所耗的人力與時間更是龐大。近年來，電腦迅速地在工商業界被採用做爲管理的重要工具，資訊系統的開發更提高了管理工作的效率，故餐飲管理的資訊系統更應配合時勢來發展其特殊功能，以便將管理工作科學現代化。

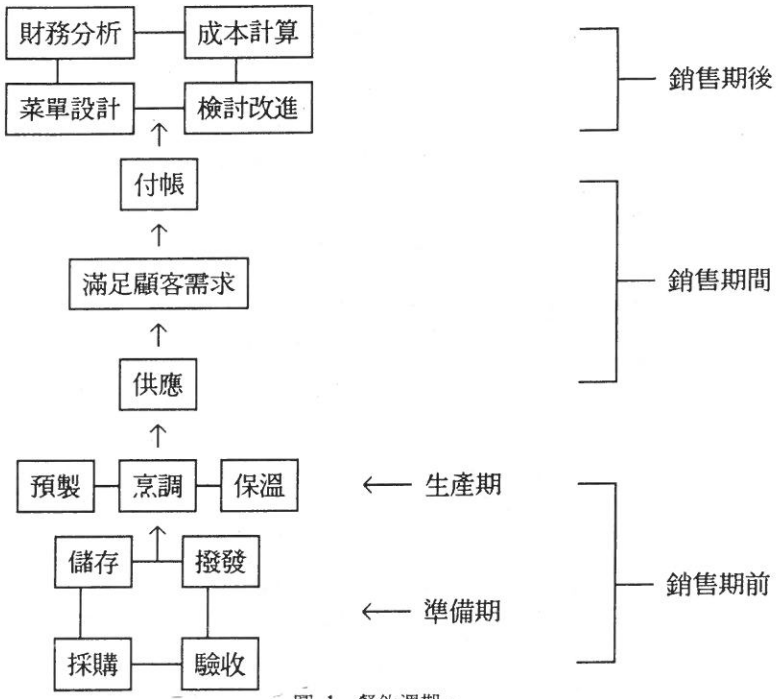

圖 1 餐飲週期。

二、設計與方法

1. 研究目的

(1) 整體系統設計完整。
(2) 各子系統可共用資料庫並相互連接。
(3) 採用中文系統作業，以方便本國學生學習使用。
(4) 採用簡易個人電腦，以普及系統使用率。
(5) 操作簡易，輸入手續明確。
(6) 輸出迅速，報表齊備。
(7) 此系統主要以教學爲目的。
(8) 此系統可推廣應用至其他學校醫院等供餐機構。

2. 系統架構

(1) 硬體系統

爲普及此系統未來的教學目標及學習使用率，在硬體設備上採用個人電腦

(Personal computer) PC-AT 型(Intel 80286-10 CPU)，並加裝 40 M 硬式磁碟機一台以充分存檔，另配備 EPSON LQ-1000C 印表機一台供報表及其他文書處理。

(2) **軟體系統**

(A) 電腦作業系統 (Operatingtsystem)：爲便利本國學生使用學習，本系統採用倚天中文系統表示；程式語言則以 dBASE III Plus 爲主。

(B) 功能子系統 (Function Subsystems) 有四部分：

(a) 庫存採購系統 (Inventory and Purchasing Subsystem)。

(b) 食物製備系統 (Food Production Subsystem)。

(c) 食物成本系統 (Food Cost Accounting Subsystem)。

(d) 飲食評估及營養分析系統 (Diet Assessment and Nutrient Analysis Subsystem)。

(C) 資料庫系統 (Data Files) 有三個：

(a) 食物種類庫 (Food Item File)。

(b) 食譜檔案庫 (Recipe Fiele)。

(c) 營養成份庫 (Nutrient File)。

3. 系統介紹

(1) **CAIFMS 整體流程**

在設計中，CAIFMS 是一個整體龐大的組織系統，爲配合餐廳業務的需求，各功能子系統之間的關係是循循相關的，在此我們可以下面圖 2 餐廳業務流程及圖 3 的 CAIFMS 流程來說明。

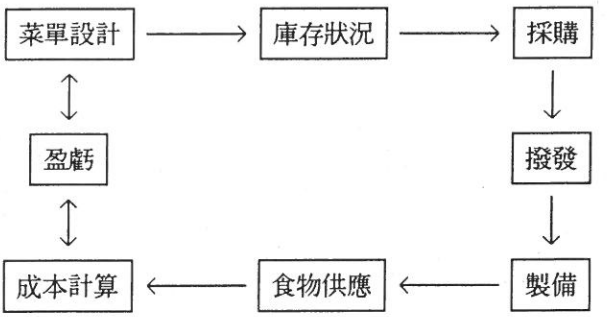

圖 2　餐廳業務流程。

在圖 2 中，餐廳經營之初，必須先對消費者的需求來設計菜單，並配合庫存狀況來做採購的工作，從採購到庫存撥發可視爲準備期，當食物正式開始製備、供應到賺取代價可視爲經營期，等交易之後，成本的計算及盈虧探討，甚至下次的菜單設計都可視爲檢討期，這就是一個供餐系統的主要生命循環。爲了配合餐廳業務的流程，CAIFMS 將以電腦取代人工的方式來從事整體業務之間的繁瑣工作，其流程如圖 3:

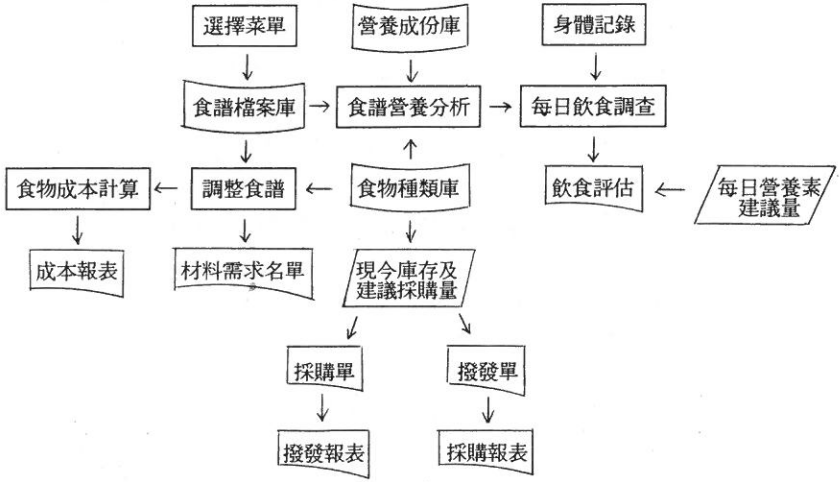

圖 3 CAIFMS 整體流程圖。

在 CAIFMS 系統中，由於標準食譜已設定成資料庫，故菜單設計亦即菜單選擇的工作，當菜單選定後，就根據供應份數來調整標準食譜的材料使用量，於是可列印出新食譜及採購單，由採購單中可先伸入到食物種類庫中查看庫存狀況，如果庫存不足則進行採購工作；如果庫存足量則進行撥發工作，事後都將有詳細的報表輸出以供查證。而新食譜的產生再配合食物種類庫中的價格數目就可以做食物成本的計算，報表的產生有助說明經營狀況及下次菜單設計的檢討工作。至於飲食評估及營養分析系統，因其較爲獨立，雖不與其他系統有直接關係，但以標準食譜的攝取量來評估個人的飲食狀況，卻可以得到更正確的分析數據，故各個子系統與資料庫之間的密切相連關係是有其意義的。

(2) 庫存採購系統介紹

在第一部份的庫存採購系統中，主螢幕爲「食物種類及採購規格」，各食物項目分類編輯成庫，且每單物均有詳細採購單位與使用單位的度量衡標示，而每單位的價格將依採購日期不同而有差異，至於波動狀況及記錄均會在各項報表中

呈現，此外，對於各項單物的供應商及進貨後的儲存地點亦有詳細的代號記錄，其目的就是對每一項的食物進出來源能把握到最充份的訊息。另一主螢幕爲「現今庫存及建議採購量」，它是針對食物種類庫所延伸的庫存狀況記錄，在這之中，我們可以瞭解每單物現有庫存量是否在最小及最大庫存量之間，如果不在安全儲存量範圍內，電腦將自動標示建議採購數量，這對庫房管理工作而言將有莫大的助益。

在圖 4 中，可以看到「採購單」及「撥發單」的輸入，由於它們主要來自各需要部門，故各單張均編號列入記錄，以爲後來報表的根源，在每日營業清點時，電腦將列印出「單日採購（撥發）報表」，由當日記錄可探知當日採購狀況，送貨情形及撥發使用地點，對於食物的進出方向能確切地把握。而在一個月末，電腦亦將列印「本月採購（撥發）總報表」，表中將比較每日記錄與所有天的平均記錄，比較本月與往月的記錄，目的在檢討食物材料的採購庫存狀況，因爲庫房是一個供餐系統中重要的財產，如果不能確切瞭解財務狀況就不能把握未來的經營方針，故各項記錄均是檢討工作中的重要依據，同時，我們對供應商的供貨情行及各使用地點的使用情行亦有記錄與比較，這對管理者而言較能做有效的控制與管理。

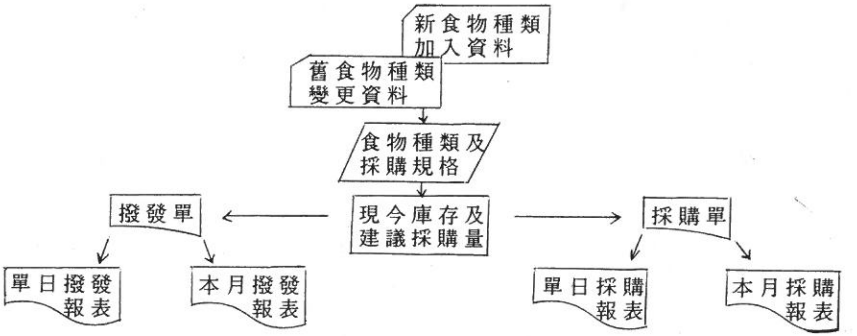

圖 4　庫存採購系統流程圖。

(3) 飯物製備系統介紹

在圖 5 中可看出最先工作卽爲選擇菜單，主螢幕爲「食譜名單」，在此我們可依材料種類、菜單種類及單份成本等選擇條件來編列標準食譜資料庫。當輸入項目包括以上各條件時，電腦就會將食譜名單中所有符合條件者顯現出來以供選擇，當輸入選擇食譜編號後，就進入「標準食譜」資料庫進行調整食譜的工作。所調整的新食譜將列印出來做爲製備時的依據，此外，若有預製工作，諸如解凍、醃製、泡水、發酵、清洗處理或與其它食譜合用者，系統亦會自動加印成爲「

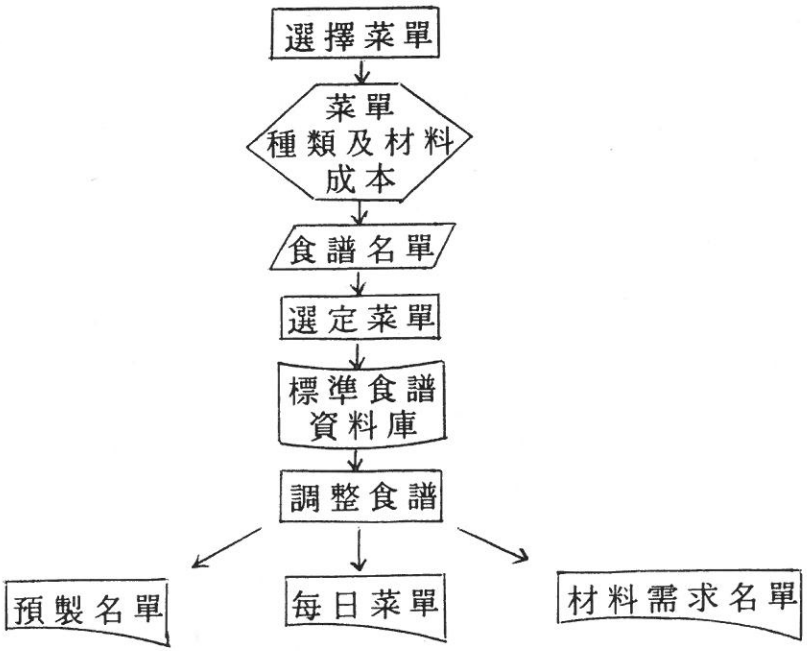

圖 5 食物製備系統流程圖。

預製名單」，指示出何種食物需此步驟，另外，亦能提供其它訊息諸如預製日期，器材溫度時間或儲存地點等等。

由於菜單設計的工作多發生在食物採購之先，故調整後的食譜能預知供應日所需材料的種類及數量。「材料需求名單」就是將各食譜中相同種類的材料相加所列印的一份材料單；這也就是在前一部份中所提「採購單」與「撥發單」的前身，在此需求名單中，詳細記錄預製日期及供應日期，如此材料可預先儲備就不會有臨時短缺的發生。

(4) 食物成本系統介紹

當菜單設計的工作完成後，新調整的食譜將會配合「食物種類及採購規格」來進行「食譜成本計算」的工作，將所需材料的數量及單價相乘相加後，就可得知此份食譜的單份成本，如果將食物成本定爲售價的百分之若干，亦可得建議售價以爲參考。在一段期限內，可依供應日期、人數、餐別、菜單種類等條件來列印出「製備成本報表」，得知在那一段時間內製備供應與成本的狀況。另一重要報表爲「單日食物成本報表」，即將各庫存採購撥發的數據依日期排列，以比較當月每日的收支狀況，而在一個月末更輸出「本月食物成本總報表」，再將上述各項條件做爲月與月之間的比較記錄。

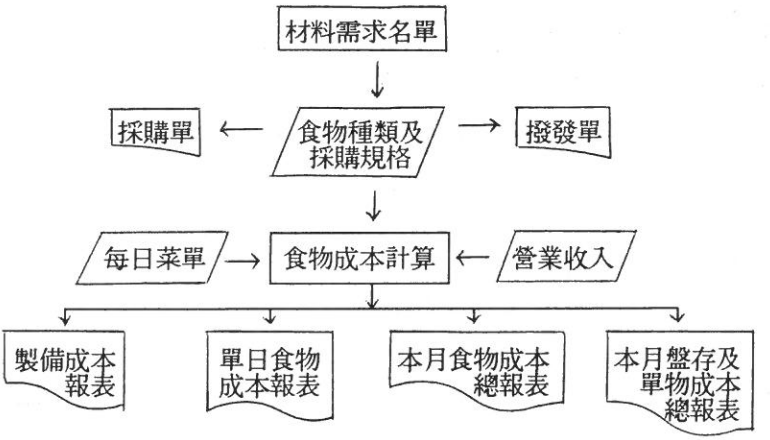

圖 6 食物成本系統流程圖。

由於庫房的存貨均可視爲餐廳的重要資產，故每月月末所做的盤存工作(Physical Inventory Check)也就是對庫房做一次清點，而記錄則稱爲「本月盤存及食物成本總報表」，表中將針對每一項食物做有系統的庫存採購分析，以得知此項食物在一個月中的消耗情形，這些數據均可做爲未來大量採購的參考指標。此系統的主要的工作就是在記錄分析食物成本的問題，唯有有效地控制成本才能繼續一個餐飲系統的生命循環。

(5) 營養評估系統介紹

雖然本系統可以算是一獨立系統，但仍需借重於食物種類庫及食譜檔案庫等兩大資料庫的資料，以完成分析工作。

首先分析各個食物的營養成份，在「食物營養成份表」中，根據食物種類庫中的各項食物編號，將18項營養成份資料輸入，以完成第三資料庫——營養成份庫(Nutrient File)；將此資料庫與食譜檔案庫相連，則可分析出各個標準食譜的單份營養含量做爲飲食的參考資料。

此外，在本系統中輸入中華民國國民每日營養素建議攝取量(RDA；衞生署)做爲另一項參考資料。當基本資料皆完整後，就可進行個人飲食評估及營養分析的工作。

在「身體記錄」功能中，輸入個人若干相關資料，如身高、體重及年齡後，電腦會算出個人應有的標準體重，再參考個人活動狀況，給予適當的營養建議攝取量，這些資料均來自於資料庫內的訊息。

在「每日飲食營養分析」中，應用食譜檔案庫的資料來調查個人每日飲食量，經過分析後再與營養建議量相比，即可得知個人在營養攝取上的過或不及做爲參考。這些工作就是本系統的主要內容，可參考圖7營養評估系統流程圖。

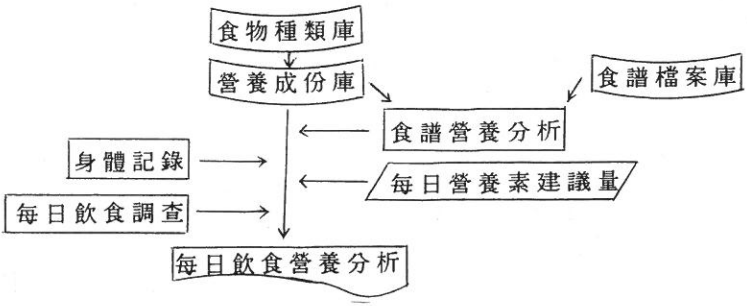

圖 7 營養評估系統流程圖。

表一 食物種類資料庫分類表

主類		子類	
F1xxx	奶蛋類	F11xx	奶製品
		F12xx	蛋製品
F2xxx	肉類	F21xx	豬肉類
		F22xx	牛肉類
		F23xx	其它家畜類
		F24xx	家禽類
		F25xx	海產類
F3xxx	豆製品	F31xx	黃豆製品
		F32xx	其它豆製品
F4xxx	蔬菜類	F41xx	甲種蔬菜
		F42xx	乙種蔬菜
		F43xx	乾菜類
		F44xx	醃菜類
		F45xx	冷凍蔬菜
		F46xx	蔬菜罐頭
F5xxx	水果類	F51xx	新鮮水果
		F52xx	醃乾水果
		F53xx	果汁類
		F54xx	水果罐頭
F6xxx	澱粉類	F61xx	米製品
		F62xx	麥製品
		F63xx	其它莖穀類
F7xxx	油脂類	F71xx	動物油脂
		F72xx	植物油脂
F8xxx	食品雜貨	F81xx	液體雜貨
		F82xx	乾性雜貨
		F83xx	酒精飲料
		F84xx	半成品食物
F9xxx	非食用雜貨	F91xx	餐用品
		F92xx	清潔用品

4. 資料庫設計

(1) 食物種類資料庫

在庫存採購系統中的「食物種類及採購規格」內，首先對各類食物做了一整套的編類系統，稱爲「食物種類資料庫」；（表一），其編號方式是以各主類爲第一位號碼，各子類爲第二位號碼，其它各個食物則依流水號來編排。各種食物均有中文與英文名字存檔以爲對照。

(2) 食譜檔案資料庫

在食物製備系統中，將各個標準食譜整理分類成庫，其編號方式亦是以各主類爲第一位號碼，各子類爲第二位號碼，其中各個食譜則依流水號來編排。由於此庫代表食譜，故以英文"R"爲標式開頭；其分類如表二：

表二 食譜檔案庫分類表

主類		子類	
R1xxx	湯類	R11xx	肉類
		R13xx	蔬菜類
		R15xx	西式
R2xxx	鹹式點心	R31xx	中式小菜
R3xxx	沙拉涼菜	R35xx	西式沙拉
R4xxx	蔬菜類	R51xx	豬肉類
R5xxx	肉類主菜	R52xx	牛肉類
		R53xx	其它家畜類
		R54xx	家禽類
		R55xx	海鮮類
R6xxx	澱粉主食	R61xx	米製品
		R62xx	麥製品
		R63xx	其它莖穀類
R7xxx	甜式點心	R81xx	果汁類
R8xxx	飲料類	R82xx	非酒精飲料
		R83xx	酒精飲料

(3) 營養成份資料庫

營養成份庫 (Nutrient File) 內的資料來自於「臺灣產常用食品之營養成份」（董大成、黃伯超等，民國七十五年），"Nuutritive Values of Selected Fast Foods"，"Mineral and Vitamin Content of Foods" (Lawier & Garwick，1986)。內容如表三：

在基本營養項目中除膽固醇是以毫克 (mg) 爲單位外，其他是以公克 (g) 爲計算單位。在礦物質與維生素項目中，除了維生素 A 是以國際單位 (I. U.) 爲單位外，其他均以毫克 (mg) 計。所有材料分析均以 100 公克爲基本分析量。

表三 營養成份庫分類表

基本營養	熱量	水份	蛋白質	脂肪	醣類	
	纖維	灰份	膽固醇			
礦物質	鈣	磷	鐵	鈉		
維生素	A	B1	B2	菸鹼酸	C	E

三、系統執行與評估

本系統的開發整整耗時2年，如今各部份電腦螢幕呈現良好，功能亦如當初之設計，報表印製十分流暢，測試可謂理想。爲了配合教學研究及學習者使用，在螢幕功能上加入相當的輔助指令以減少對使用手册的依賴性。雖然在設計上，完全以標準的餐飲經營理念爲依歸，但其確實的使用效果，仍有待歲月及業者的考驗，相信不停的測試與修正應是本系統未來永不停止的工作。

四、致　　謝

在此感謝輔仁大學理工學院聖言會單位給予本研究的肯定與經費支助，致使此系統能順利完成，並於日前申請到內政部的著作權執照（執照字號：台內著字第81736號），所有權歸輔仁大學。

此外，要感謝柏殿宏院長的支持鼓勵，及本校數學系黃文祥老師的推薦，才得與數學系畢業高材生陳文龍共同合作編寫程式，順利將此系統開發完成，在此亦表示最深的謝意。

參考資料

(1) J. Chaban, Practical Foodservice Spreadsheets with Lotus 1-2-3 Van Nostrand Reinhold Company Inc., New York (1987).
(2) L.W. Hoover and A.N. Moore, Dietetic Com-Pak Student Guide, Locas Brothers Publishers, Los Angeles (1978).
(3) M.L. Kasavana, Computer System for Foodservice Operations, Bookwrights Inc., Wakefield MA (1988).
(4) M.L. Kasavana and J.J. Cahill, Managing Computers in the Hospitality Industry, Educational Institute of the American Hotel and Motel Association, Michigan (1987).
(5) R.G. Murdick and J.E. Ross, Introduction to Management Information System (1977).
(6) J. Orta, Computer Applications in Nutrition ane Dietetics, an Annotated Bibliography, Garland Publishing Inc., New York (1988).

(7) C.A. Sawyer, CBORD Foodservice Management System, East Lansing, Michigan State University (1984).
(8) The 1987 Proceedings of the Computer Application in Foodservice Education Society, The CBORD Group Inc., Ithaca, N.Y. (1988).
(9) 陳程光、程嘉君譯，系統分析與設計，松崗圖書公司（民國73年）。
(10) 于厚澤譯：資料庫處理，儒林圖書公司（民國75年）。
(11) 瑩圃電腦軟體研究開發部門編譯，CLIPPER 使用與程式設計手册，尖端電腦雜誌（民國77年）。
(12) 黃韶顏，自助餐菜單的設計，圓山圖書公司（民國75年）。

Computer-Assisted Instruction in Foodservice Management System

JONG-YU CHYUAN
Applied Life Science Departmemt
Fu-Jen Catholil University

ABSTRACT

For the purpose of assessing the effecttiveness of computer assisted management with foodservice works, a computer-assisted instruction (CAI) in foodservice management system has been developed. Althought the original CAI design was placed into the educational framework, it also can be tested determine whether their functions can meet the purposes of each hospital or school foodservice practical works.

The main system consists of four subsystems covering the following functions:

1. Inventory and Purchasing Control Subsystem: Food item and purchase specification, inventory amount and recommended purchases, purchase order, issue order, daily report of purchase and issue, monthly summary of purchase and issue.
2. Food Preparation Control Subsystem: Menu list, standarized recipe, menu sorting and combination, adjusted recipes, advanced preparation list, advanced ingridients requisition.
3. Food Cost Analysis Subsystem: Recipe cost analysis, food preparation cost reports, daily food cost reports, monthly summary

of food cost, physical inventory report with food item cost.

4. Diet Assessment and Nutrient Analysis Subsystem: Nutrient composition of foods, recipe nutrient analysis, personal body record and nutrients intake recommendation, personal daily diet assessment.

The CAIFMS program was developed with Chinese system on a personal computer (PC) for easy operation. A licence from the Copyright Committee of the Ministry of Interior (ROC) has been acquired. The intented goals are not only to implement the education purposes but also to integrate this program into a dietetic works.

FACTORS AFFECTING THE STALING OF BREAD: A REVIEW

B. H. CHEN

Department of Nutrition and Food Science
Fu Jen University
Taipei, Taiwan 24205, R.O.C.

ABSTRACT

Bread staling, although researched for many years, has not been solved. This paper reviews the role of various flour constituents, surfactants and baking procedures on the staling of bread. Staling is characterized by starch retrogradation at room temperature. Some other factors such as protein denaturation and moisture redistribution play an important role at higher temperature because less crystallization of starch occurred at higher temperature. Amylose contributes to staling during the first day of storage; and thereafter, the staling is controlled by the amylopectin fraction of starch. Also the role of amylose in staling diminishes as the protein content increases. The higher storage temperature and higher protein content decrease the staling rate. The primary effect of protein in reducing staling rate might be due to dilution of the starch and not the quality of the protein. Surfactants complex with the amylose fraction of starch and thus decrease firmness of bread. Bread prepared by the continuous-mix baking procedure tended to change less in soluble starch and amylopectin as the bread aged when compared with bread prepared by the conventional baking procedure. The difference might be due to baking procedures or baking formulas.

1. INTRODUCTION

Bread staling, a major problem in the baking industry, can cause considerably economical loss to both the industry and the consumer. The consumer's demand for fresh bread causes the industry to withdraw all bread from the market after it becomes two days old. Currently, stale bread returns in the industry are in the order of about 7.5 to 9.5% of production[1]. Therefore, bread staling has become an urgent problem to solve in the baking industry.

Bread staling is an extremely complex phenomenon and is difficult

to define in straightforward terms. According to Bechtel et al.[2], staling can be defined as "a term which indicates decreasing consumer acceptance of bakery products caused by changes in the crumb other than those resulting from the action of spoilage organisms". Broadly speaking, bread staling refers to all changes that occur in both the crumb and the crust of the bread after baking. The increase in crumb firmness, starch crystallinity and opacity, decrease in water absorption capacity, amount of soluble starch and enzyme susceptibility of the starch, loss of flavor and changes in X-ray diffraction pattern are changes occurring during the staling of bread.

Since the major component of bread is flour, flour quality has been acknowledged as a factor in the keeping quality of bread. Flour consists predominantly of a mixture of proteins (gluten), starch and water in the approximate ratio of 1:6:5[3]. In addition, pentosans and lipids are also present in small amounts. Therefore, the staling phenomenoa might be considered in terms of changes among these components. Wall[4] reported that some transitional compounds such as glycoproteins, glycolipids and lipoproteins do exist in wheat flour in addition to proteins, carbohydrates, and nonpolar lipids. These transitional compounds permit physical association and chemical bonding between the major components and thus might play an important role in bread staling. The purpose of this paper is to review the role of various constituents of wheat flour in bread staling with emphasis on the role of surfactants and baking procedures.

2. THE ROLE OF STARCH

Numerous studies designed to determine the cause of bread staling have indicated that changes in starch play a major role in causing bread firmness. Cornford et al.[5] studied the relationships between elastic modulus, time and temperature in bread crumb, on the assumption that the increase in crumb modulus is proportional to the growth of crystallinity of the starch. These workers found that the rate of bread firming could be described quantitatively by the Avrami equation: $\theta=\exp(-kt^n)$ where θ is the fraction of uncrystallized material remaining after time t, k is a rate constant and n is the Avrami exponent

whose value varies from 1 to 4 depending on the mode of nucleation of the starch (Table 1).

Table 1. Values for the avrami exponent for various types of nucleation and growth[6]

n*	Types of nucleation and growth
3+1=4	Spherulitic growth from sporadic nuclei
3+0=3	Spherulitic growth from instantaneous nuclei
2+1=3	Disc-like growth from sporadic nuclei
2+0=2	Disc-like growth from instantaneous nuclei
1+1=2	Rod-like growth from sporadic nuclei
1+0=1	Rod-like growth from instantaneous nuclei

* n is a combined function of the number of dimensions in which growth takes place, and the order of the time dependance of the nucleation process (0 or 1).

Bread crumbs were stored at temperatures from −1 to 32°C (30-90°F). These workers observed that the relative rate of increase in limiting elastic modulus became greater as storage temperatures were lowered towards the freezing point. Thus, the evidence emphasized the importance of crystallization, a physical process involving a more ordered arrangement of molecules, was the principal factor involved in crumb firmness. Table 1[6] shows that the basic mechanism of retrogradation of starch is instantaneous nucleation followed by the rod-like growth of crystals while the value for the Avrami exponent is equal to 1.

Table 2[6] shows that data for the Avrami exponent and the time constant for bread and starch gels are in good agreement. The time constant is the time for any given fraction of material to be converted to the stale form. These data thus indicate that bread staling is basically characterized by the retrogradation of the starch component of the crumb. Wright[7] compared bread firmness with crystallinity of starch by X-ray diffraction and found that, for a given firmness measured at room temperature, there was a higher level of crystallinity for bread stored at 4°C than 21°C. This result demonstrates that the firming of bread at constant moisture levels is controlled by the degree

Table 2. Comparison of avrami exponent and the time constant of bread and 50 per cent starch gels stored at 21°C[6]

	Avrami exponent	Time constant (days)
Starch gel	1.02	3.76
Starch gel	0.90	4.20
Starch gel	0.98	3.80
Bread[1]	1.00	3.68
Bread[2]	—	3.28

[1] Conventional baking process.
[2] Chroleywood bread process.

of crystallinity of the starch. However, Neukom and Rutz[8] found that starch retrogradation was more evident with bread from corn starch and a wheat starch/waxy corn starch mixture than the other breads. Thus the authors concluded that there was no clear relationship between retrogradation and staling. Dragsdorf and Varriano-Marston[9] studied the effects of bareley malt, fungal α-amylase and bacterial α-amylase on starch crystallization in staling bread by X-ray diffraction. They compared X-ray patterns of fresh and stored breads and found that the degree of starch crystallinity were in direct contradiction to bread firming data. This result suggested that starch crystallinity and bread firming were not synonymous. Thus the role of starch crystal structure in bread firming should be further investigated.

3. THE ROLE OF AMYLOSE AND AMYLOPECTIN

Although the firming of bread is believed to be due to the crystallization of starch fraction, it has not been established which of the two starch fractions is responsible for staling. Schoch[10] reported that the hardening of crumb structure during staling was due to the amylopectin fraction within the swollen granules. The author proposed that the starch granules underwent swelling during baking, which in turn caused a portion of the linear fraction to dissolve and diffuse out of the granule into the surrounding aqueous medium. As the granule continued to swell, these linear molecules became concentrated in the

small amount of interstitial water between the starch granules. This would result in the retrogradation of the linear molecules and set up a permanent gel network between granules by the time the loaf is cooked. Rusch[11] reported that upon cooling, the amylose polymers associated with each other through hydrogen bonding and formed a rigid gel within 10-12 hours. The amylopectin crystallized more slowly and resulted in the "staling" or firming of bread over a period of 3-6 days. However, Maga[12] found that the changes in bread staling were due to modifications in the amylose fraction. This result seems to be contradictory to those results reported by previous workers. This problem is further clarified by Kim and D'Appolonia[13] who demonstrated that the crystallization of starch gels is characterized by the retrogradation of both amylose and amylopectin over the first day of storage, after which amylopectin alone controls the retrogradation process. This result also indicate that storage temperature also plays an important role in controlling starch crystallization. Kim and D'Appolonia[14] examined the effect of staling on the quantity and composition of soluble starch extracted from bread crumb during storage (Table 3). The amount of amylose in the soluble starch leached from the bread crumb after 0.16 hr of cooling is small, but a sharp decline in the amylose content occurs during the 5 hr cooling period after baking. This implies that the amylose contributes to staling primarily during the first day of storage. However, firmness data on refreshened bread showed that the staling of bread at 21°C was due primarily to starch crystallization. At 30 and 35°C, some other factors

Table 3. Effect of staling on the quantity and composition of soluble starch extracted from bread crumb during 12 hr of storage[14]

Time (hr)	Storage temperature (°C)	Soluble starch (%)	Composition of soluble starch	
			Amylose (%)	Amylopectin (%)
0.16	Room temperature	2.51	0.60	1.91
2	Room temperature	2.34	0.39	1.95
5	21	1.86	0.22	1.64
12	21	1.74	0.18	1.56

played an important role in firming. Since less crystallization of starch occurred at higher temperature, other factors such as protein denaturation or moisture redistribution might be involved in the firming process. This needs further investigation.

4. THE ROLE OF PROTEINS

Numerous reports have shown that flour protein content is an important factor in controlling the rate of bread staling. Bechtel and Meisner[15] and Prentice et al.[16] found that increasing the protein level of the synthetic flours decreased the average crumb firmness and crumb firming rate. However, Ponte et al.[17] reported that the rate of bread firming was not significantly correlated to flour protein content. Erlander and Erlander[18] reported that the ratio of starch to protein in the dough is critical in determining the rate of staling, and some staling will always occur no matter how much protein is present in the dough. They also postulated that the retrogradation of starch might be inhibited by the formation of a complex with the protein of bread, and proposed that the amide groups of wheat gliadin and glutenin were hydrogen bonded to the hydroxy groups of starch. Data present in Table 4[6] shows that the staling rate of bread dereases as the protein content of increases. However, the values for the Avrami exponent indicated that the basic mechanism of bread staling is not affected by the protein quality. It is because the time constants were similar for the breads produced from flours of different strength but the same protein content, suggesting that the staling rate of bread is independent of protein quality. Therefore, the results in Table 4[6] suggest that the primary effect of protein in reducing the staling rate is dilution of the starch and not the quality of protein. This result supports Erlander and Erlander[18], who emphasized the importance of the ratio of starch to protein in the dough in determining the rate of bread staling. Kim and D'Appolonia[14] investigated the effect of flour protein content and storage temperature on the role of starch during bread staling. The recovery of soluble starch extracted from bread crumb was inversely and positively related to the protein content of the flour and storage

Table 4. Effect of protein content of flour on avrami exponent and time constant of bread stored at 21°C[6]

Flour		Bread	
Protein content (%)[1]	Stability (min)[2]	Avrami exponent	Time constant
10.6	12.5	0.94	3.75
11.0	5.5	0.92	3.74
13.9	16.0	0.92	5.44
21.6	21.0	1.04	11.25

[1] On a 14 per cent moisture basis (N×5.7).
[2] Farinograph data.

temperature, respectively. The soluble starch from fresh crumb was predominantly amylopectin, which progressively decreased as bread aged. Although the amylose content in the soluble starch was small, it sharply decreased during the first day of storage and thereafter the changes were minor. The amylose was essentially absent in the soluble starch leached from the bread produced from the flour with the highest protein content, suggesting that the role of amylose in staling diminishes as the flour protein content increases. Maleki et al.[19] determined the effect of protein quality on the softness and staling rate of bread. They found that increasing the protein content of flour increased the loaf volume and resulted in softer bread. Four varieties of wheat were milled and two of the flours were fractioned into gluten, starch, and water solubles. Breads were baked from original flours and from reconstituted flours with or without interchanging the fractions. The protein contents of Eagle, NE 69774, Omaha, and Aurora were 13.2, 13.1, 14.0 and 12.1%, respectively. Table 5[19] reports staling rates of breads from various flour samples. Values for the four original flours showed that the flour of Eagle wheat produced bread that staled most slowly and of NE 69774, most quickly. Reconstitution of starch and water solubles from NE 69774 with the gluten from Eagle gave a reconstituted flour that staled at a rate equal to reconstituted Eagle. Therefore, the starch and water-soluble fractions from the two different flours did not significantly affect the staling rate. However, when the gluten fractions of NE 69774 was replaced with the gluten of Eagle,

Table 5. Staling rates of breads from various flour samples[19]

Flour	Bread sampled after					
	1 hr		1 day		3 days	
	PU[1]	% PU[2]	PU	% PU	PU	% PU
Original:						
Eagle	184	100	125	68	91	49
NE69774	169	100	97	57	61	36
Omaha	177	100	108	61	78	44
Aurora	163	100	95	58	59	36
Reconstituted:						
Eagle	187	100	127	68	88	47
NE69774 with eagle gluten	204	100	125	61	86	42
Eagle with NE69774 starch	189	100	133	70	93	49
Eagle with NE69774 water solubles	184	100	122	66	83	45
Standard deviation	7.8		7.1		7.4	

[1] Penetrometer units.
[2] Percent of original PU indicates staling rate.

reconstituted NE 69774 flour's staling rate improved and approached that of Eagle flour. This indicated that the flour component primarily responsible for differences in staling rate of these two flours was the gluten fraction. This finding is contrary to the views of many workers, who reported that the primary effect of protein in reducing staling rate was its dilution of starch. The difference might be due to flours from different varieties of wheats and quality of protein.

5. THE ROLE OF PENTOSANS

Pentosans, which are polysaccharide materials, are a minor component of wheat flour present at the 2-3% level. Of the total pentosans, about one half are extractable with water and the remaining portion, the "water-insoluble pentosans" are extracted with alkali; however, once extracted, they are water-soluble. It has been reported[20] that the water-soluble pentosans present in the "soluble starch" extracted from fresh bread crumb inhibited the retogradation of amylose. How-

ever, the water-soluble pentosans did not affect the staling rate. Wall[4] postulated that pentosans and glycoproteins were present as transitional compounds, permitting physical association and chemical bonding between carbohydrates and proteins. Patil et al.[21] found that the mixing of flour into dough caused a conformational change in water-soluble pentosan molecules, which in turn intensified the association between carbohydrates and protein constituents. Whether the water-insoluble pentosans play a similiar role is unknown. Kim and D'Appolonia[13] studied the association between pentosans and starch by using starch, starch-amylose, and starch-amylopectin gels, with or without the addition of pentosans. Figure 1[13] shows the effect of pentosans on firming of starch gels. Pentosans had a definite effect on retarding starch retrogradation, with the effect exerted by the water-insoluble pentosans being more pronounced than that by the water-soluble pentosans. Table 6[22] shows the effect of pentosans on the staling rate of bread at 21°C. Pentosans increased the time constant of the bread, with the effect exerted by the water-insoluble pentosans being more pronounced than

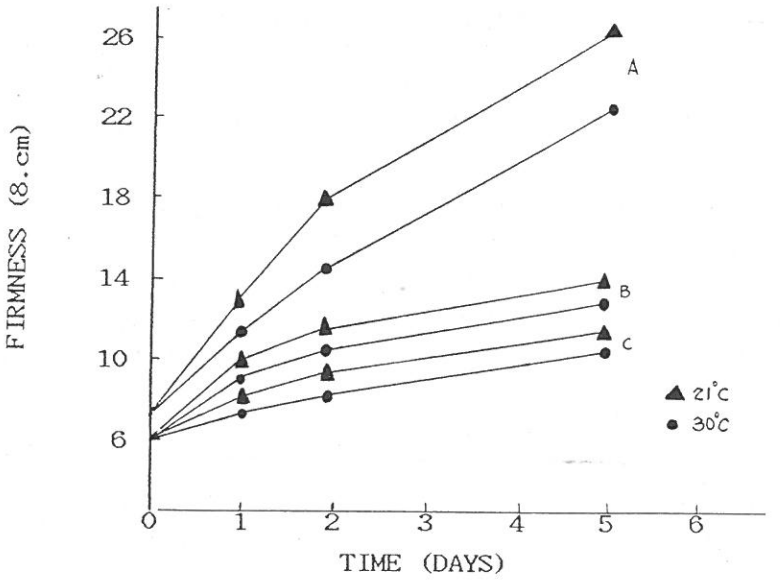

Fig. 1. Aging of starch gels (A) and starch-soluble (B) and starch-insoluble (C) pentosan gels at 21 and 30°C[13].

Table 6. Effects of pentosans on the time constant of bread stored at 21°C[22]

Bread	Time constant (days)	
	Overall	Over the first day storage
Control	5.44	4.80
With 1.0% soluble pentosans	6.53	4.23
With 1.0% insoluble pentosans	8.54	5.88

that exerted by the water-soluble pentosans. Kinetic studies by Kim and D'Appolonia[22] indicated that pentosans simply reduced the amount of starch components available for crystallization, thus decreased the bread staling rate. Jankiewicz and Michniewicz[23] studied the effect of soluble pentosans isolated from rye grain on staling of bread. They found that starch in test bread had greater resistance to retrogradation, and the extented shelf-life of bread was due to the increased pentosan content and the starch-pentosan interaction.

6. THE ROLE OF MOISTURE

It has been known that bread does not necessarily lose moisture during staling. Stale, firm bread often contains as much moisture as does fresh, soft bread. Part of the water is thermodynamically bound and part is distributed in the intermolecular spaces of the protein and partially swollen gelatinized starch[6]. It is generally believed[2,23] that increasing water absorption in bread dough enhances softness and retards firming. Moisture redistribution between components during bread storage has been a controversial subject. Senti and Dimler[24] reported that moisture transfer would occur from the starch to the gluten in the crumb during aging, whereas Willhoft[25] found a moisture transfer from gluten to the starch took place. Since the hardening of gluten due to moisture loss in bread staling is most likely to happen, a transfer of moisture from gluten to starch gel is quite possible. Verbii et al.[26] also found that the degree of staling and rate of moisture loss were directly proportional. Neukom and Rutz[8] demonstrated that higher moisture content and larger loaf size produced

softer bread. However, bread crumb has an equilibrium relative humidity of 97% and an open structure[27], both may be important in the study of moisture transfer between components.

7. THE ROLE OF LIPIDS

The studies conducted on flour lipids have been concerned primarily with their functional properties in bread baking. It has been shown that the role of lipids in baking is primarily the enhancement of loaf volume, which is negatively related to bread staling. It is generally agreed that the polar lipids have an improving effect on the volume of bread baked from defatted flour but nonpolar lipids have a detrimental effect on this bread property[6]. Pomeranz et al.[28] studied the compressibility of bread to which vegetable shortening and nonpolar, polar, and total lipid fractions from six wheat flours were added. Adding 0.5 g of nonpolar lipids per 100 g of wheat flour reduced crumb firmness only slightly. For significantly retarding firmness of crumb during storage, 0.5 g of polar lipids were as effective as was 3 g of shortening. Verbii et al.[25] also found that breads containing fat and phosphatide concentrate could reduce crumb firmness. Wehrli and Pomeranz[29] reported that a complex between glycolipids and starch was apparently significant and could be responsible for the improved freshness retention of bread baked with glycolipids. Surfactants might also play an important role in interaction with lipids. Thus, the possible importance of interaction among various components and their effects on bread staling should be examined further. What effects do the lipids in the starch granule, although present in small amounts, have on bread staling?

8. THE ROLE OF SURFACTANTS AND BAKING PROCEDURES

Surfactants are used as crumb softening agents or antifirming agents by interacting with starch, particularly the linear amylose fraction of starch. This can be demonstrated by the presence of the V diffraction pattern by X-ray deffraction studies[30]. The some pattern

arises from the interaction of a surfactant with the proper geometry with the tight α-helix of the amylose. The helix, with its inner diameter of 4.5-4.6 Ångstroms, can only accommodate a surfactant whose diameter is less than 4.5 Ångstroms. In contrast, retrograded starch which has an extented configuration produces a B diffraction pattern. The two starch structures, represented by V and B patterns, do not co-crystallize. Table 7[27] shows that bread containing surfactants has a consistently higher line intensity for the V pattern and is also softer and has less B crystallinity than the control without an additive. From the differences in the intensity of the diffraction patterns in the bread containing surfactants and of bread without additives, the conclusion can be drawn that amylose in the helical configuration interferes with the crystallization of the extended starch chains which are typical of retrograded starch.

Surfactants can be adsorbed onto the surface of the starch granules and prevent the gelatinized starch granule from binding together and delay the swelling process. The degree to which this effect depends on

Table 7. X-ray analysis of breads made with surface-active agents[27]

Bread No.	Description of additives	Compression data[1]	Intensity of diffraction lines[2,3]			Complexing index[4]
			Structure	B	V	
1	Control	13.8	B>V	10	7	—
2	Hydrated mono-diglyceride, 20%	12.1	B<V	6	10	28
6	Succinylated monoglyceride	11.8	V>B	6	9	63
4	60% mono-di, 40% ethoxylated monoglycerides	11.6	V>B	5	9	30
3	Sodium stearoyl-2-lactylate	10.6	V>B	4	10	72
5	75% Hydrated mono-diglyceride, 25% Polyoxethylene sorbitan 20	10.5	V>B	4	10	29

1) After three days' aging.
2) After six days' aging.
3) Scale, 1-10 with 10 being the most intense; B, retrograded starch structure; V, amylose complex structure.
4) Adjustments made for composition.

the chemical composition of the surfactant and on the structure of the hydrophilic moiety, the length of chain, and the degree of saturation of the lipophilic parts[31]. Birnhaum[32] reported that surfactants reduced the effective concentration of moisture in the starch phase and increased the moisture retention of the gluten, tying up moisture in the bread crumb. Although numerous studies on the role of surfactants in retarding firmness have been published, the mode of their action in improving the shelf life of bread has been controversial. Schoch[10] suggested surfactants could form a complex with amylose, resulting in softer crumb but without influencing the firming rate. Other workers reported that surfactants had little or no effect on initial bread crumb firmness but did affect the firming rate during storage[33]. Krog[34] proposed that surfactants might slow the rate of bread firming by forming a complex with the amylopectin fraction within the starch granule. De Stefanis et al.[35] reported that a crumb softener formed a complex with both the amylose and the amylopectin fraction of starch in bread. Since surfactants of different chemical structures differ widely in their effect on crumb firmness, the ionic surfactants such as sodium-stearoyl-lactylate (SSL) and the nonionic surfactants such as ethoxylated monoglyceride (EMG) form two different kinds of macromolecular complexs[30]. SSL forms aggregates consisting of a coupled complex "protein-starch complex" as shown in Fig. 2[30]. In this complex, the anionic lactylates serve as ligands with the glutenin and starch as well as with the gliadin. The polar lipids and the ionic SSL mediate between these flour components. In contrast, the nonionic EMG forms a stable "protein complex" as shown in Fig. 3[30]. Since the SSL and EMG

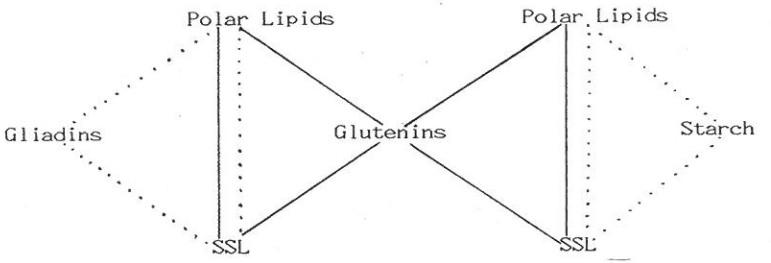

Fig. 2. Protein complex-starch complex with ionic (SSL) surfactant[30].
—— hydrophobic bonds, ····· hydrophilic bonds

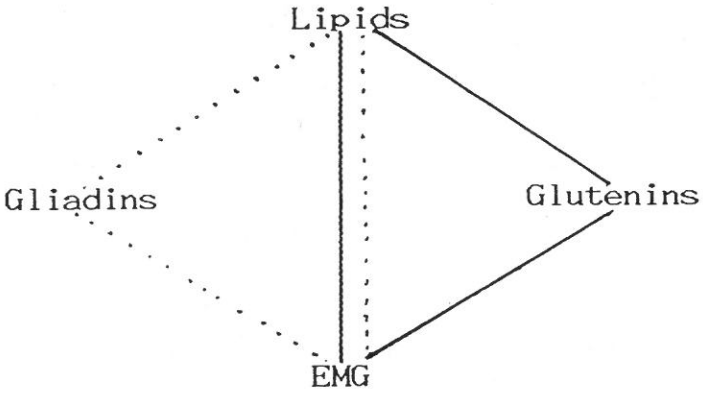

Fig. 3. Protein complex with ethoxylated monoglycerides and lipids[30].
—— both hydrophobic and hydrophilic bonds with hydrophobic predominating
..... both hydrophobic and hydrophilic bonds with hydrophilic predominating

differ in their electric charge and therefore form different types of complexs, the action of the surfactants in breadmaking is different. The lactylates (SSL), which are able to integrate starch and gluten into one complex, produce loaves with a slower firming rate than those obtained with EMG. The addition of EMG produces a larger loaf volume because the gluten can be developed unimpeded due to the absence of starch in the "protein complex".

Morad and D'Appolonia[36,37] determined the effect of surfactants and baking procedures on the pasting properties and total water-solubles and soluble starch in bread crumb. The effect of baking process was examined by using the conventional straight dough and the continuous-mix baking procedure. The pasting temperature did not change greatly with longer storage time, but it increased with the incorportion of surfactant. Also pasting temperatures for the bread crumb obtained by the continuous-mix baking procedure were higher than those obtained with the straight dough procedure. The amount of soluble material extracted from the conventionally made bread was less than that from the continuous-mix bread. The values for amylose in the soluble starch were lower for the continuous mix than for the conventionally baked bread, which could be a result not only of the type of processing but

also difference in formulation. Extracts of bread crumbs containing surfactants and made by either baking procedure contained less amylose than did the control bread crumb, whether measured in the total soluble material or in the soluble starch. The data indicated that amylose and the surfactant formed a complex that varied among surfactants. However, the effect of surfactant components and different baking formulas used in straight dough and continuous-mix baking procedures on the water-solubles and soluble starch in bread crumb should be further investigated.

Pisesookbunterng and D'Appolonia[38] investigated the effect of surfactants on moisture migration from crumb to crust and firmness values of bread crumb. In bread containing surfactant, moisture migration from the crumb to the crust was greater than in the control bread. This is probably because the level of surfactant used in bread-making, 0.5%, does not lower surface tension of water in bread crumb, and thus can not assist in moisture retention within the crumb. Also the adsorption of surfactant onto the starch surface, as well as the complex formation between starch and surfactant, prevent starch from taking water released from gluten during bread aging. However, the authors found that surfactants did not affect firmness of fresh bread crumb, but did slow the firming rate of bread crumb during bread storage. This result conflicts with those previous workers who found that surfactants gave a softer bread crumb in fresh bread but did not influence the firming rate. The difference might be due to various kinds of surfactants, baking formulas, and experimental procedures. Moreover, the authors suggest that the concentration of surfactants should exceed 1% in order to maintain the higher moisture contant. This needs further investigation.

In a later study, Pisesookbunterny et al.[39] evaluated the role of refreshening in bread staling. Breads stored at 2 and 30°C were refreshened by heating at 90°C for 45 min. Those stored at 2°C for 2 days and refreshened regained the original firmness. Surfactants (SSL and Atmul 500) were found effective in restoring original freshness of breads. Hansen et al.[40] further demonstrated that resistant starch was formed during baking and that the chemical composition of bread was not significantly affected by staling.

REFERENCES

(1) J.G.Jr. Ponte, *American Assocation of Cereal Chemists*, 675 (1971).
(2) W.G. Bechtel, D.F. Meisner and W.B. Bradley, *Cereal Chem.*, **30**, 160 (1953).
(3) E.M.A. Willhoft, *Bakers Dig.*, **47**, 14 (1973).
(4) J.S. Wall, *Cereal Sci. Today.*, **16**, 412 (1971).
(5) S.J. Conford, D.W.E. Axford and G.A.H. Elton, *Cereal Chem.*, **41**, 216 (1964).
(6) S.K. Kim and B.L. D'Appolonia, *Bakers Dig.*, **51**, 38 (1977).
(7) W.B. Wright, Paper Presented at the S.C.I. Food Group Symposium on Starch: Granule Structure and Technology, *London* (1971).
(8) H. Neukom and W. Rutz, *Lebens-Wissens-Tech.*, **14**, 292 (1981).
(9) R.D. Dragsdorf and E. Varriano-Marston, *Cereal Chem.*, **57**, 310 (1980).
(10) T.J. Schoch, *Bakers Dig.*, **39**, 48 (1965).
(11) D.T. Rusch, *Cereal Foods World.*, **26**, 111 (1981).
(12) J.A. Maga, *Crit. Rev. Food Technol.*, **5**, 443 (1975).
(13) S.K. Kim and B.L. D'Appolonia, *Cereal Chem.*, **54**, 150 (1977).
(14) S.K. Kim and B.L. D'Appolonia, *Cereal Chem.*, **54**, 216 (1977).
(15) W.G. Bechtel and D.F. Meisner, *Cereal Chem.*, **54**, 216 (1954).
(16) N. Prentice, L.S. Cuendet and W.F. Geddes, *Cereal Chem.*, **31**, 188 (1954).
(17) J.G.Jr. Ponte, S.T. Titcomb and R.H. Cotton, *Cereal Chem.*, **39**, 437 (1962).
(18) S.R. Erlander and L.G. Erlander, *Staerke.*, **21**, 305 (1969).
(19) M. Maleki, R.C. Hoseney and P.J. Mattern, *Cereal Chem.*, **57**, 138 (1980).
(20) K.A. Gilles, W.F. Geddes and F. Smith, *Cereal Chem.*, **38**, 229 (1961).
(21) S.K. Patil, C.C. Tsen and D.R. Lineback, *Cereal Chem.*, **52**, 57 (1975).
(22) S.K. Kim and B.L. D'Appolonia, *Cereal Chem.*, **54**, 225 (1977).
(23) M. Jankiewicz and J. Michniewicz, *Food Chem.*, **25**, 241 (1987).
(24) F.R. Senti and R.J. Dimler, *Bakers Dig.*, **34**, 28 (1960).
(25) E.M.A. Willhoft, *J. Texture Stud.*, **4**, 292 (1973).
(26) V.P. Verbii, A.P. Demchuk and N.A. Chumachenko, *Tovarovedenie.*, **17**, 47 (1984).
(27) H.E. Zobel, *Bakers Dig.*, **47**, 52 (1973).
(28) Y. Pomeranz, G.L. Rubenthaler, R.D. Daftary and K.F. Finney, *Food Tech.*, **20**, 131 (1966).
(29) H.P. Wehrli and Y. Pomeranz, *Cereal Chem.*, **47**, 216 (1973).
(30) H. Birhaum, *Bakers Dig.*, **51**, 16 (1977).
(31) E.M. Osman and M.R. Dix, *Cereal Chem.*, **37**, 464 (1960).
(32) H. Birhaum, *Bakers Dig.*, **29**, 46 (1955).
(33) C.W. Ofelt, M.M. Macmarten, E.B. Lancaster and F.R. Senti, *Cereal Chem.*, **35**, 137 (1958).
(34) N. Krog, *Staerke.*, **23**, 206 (1971).
(35) V.A. Destefanis, J.G.Jr. Ponte, F.H. Chung and N.A. Ruzza, *Cereal Chem.*, **54**, 13 (1977).

(36) M.M. Morad and B.L. D'Appolonia, *Cereal Chem.*, **57**, 141 (1980).
(37) M.M. Morad and B.L. D'Appolonia, *Cereal Chem.*, **57**, 239 (1980).
(38) W. Pisesookbunterng and B.L. D'Appolonia, *Cereal Chem.*, **60**, 298 (1983).
(39) W. Pisesookbunterng, B.L. D'Appolonia and K. Kulp, *Cereal Chem.*, **60**, 301 (1983).
(40) H.B. Hansen, K. Osterguard and K.E.B. Kundsen, *J. Cereal Sci.*, **7**, 135 (1988).

影響麵包老化的因素：文獻回顧與探討

陳　炳　輝

輔仁大學食品營養系

摘　要

麵包老化的現象已經被研究了許多年，可是到目前爲止仍無法完全回答這個問題。本文主要在回顧及討論影響麵包老化的因素。麵包老化的特性卽是指澱粉在室溫下會產生回凝的現象，其他的因素例如蛋白質的變性和水分的重新分布則對在高溫下產生麵包老化的現象較有重要的影響，因爲澱粉在高溫下產生結晶化的現象較少。麵包於第一天貯藏時所產生的老化現象是由直鏈澱粉所控制，第二天以後則由支鏈澱粉所控制，可是當蛋白質含量增加時，直鏈澱粉對麵包老化的影響則變小；較高的貯藏溫度及蛋白質含量都會減低麵包老化的速率，蛋白質會降低麵包老化速率可能與澱粉的被稀釋有關係。界面活性劑會與直鏈澱粉結合進而減少麵包硬化的現象。由連續混合式烘焙方法及由傳統烘焙方法所製造出來的麵包於室溫老化時，前者對於麵包中可溶澱粉及支鏈澱粉的改變較少，這個不同點可能與烘焙步驟與配方有關。

MENADIONE-INDUCED CARDIOTOXICITY IN CULTURED NEONATAL CARDIOMYOCYTES

WOAN-FANG TZENG AND JEN-YEE HUANG

Department of Biology
Fu Jen University, Taipei, R.O.C.

ABSTRACT

Isolated neonatal rat cardiomyocytes were used to study the cardiotoxicity of menadione. Menadione inhibited the beating of the cells in a time and dosage dependent manner. At high menadione dose, 80 uM, cessation of beating was rapid and occurred within 30 min. The cells were killed at higher dosages or with longer incubation time. Cardiomyocytes incubated with ^{35}S-methionine were used to study the inhibition of protein synthesis and the expression of stress proteins in response to heat shock or exposing to menadione. Menadione treatment resulted in a decrease in protein synthesis in a time and dosage dependent manner. One hour heat shock at 42°C depressed the protein synthesis of cardiomyocytes. Heat shock protein 70 was induced in cells exposed to heat shock (42°C, 60 min), but it was not induced when cells were exposed to menadione.

Our results indicate that menadione is cardiotoxic to cardiomyocytes, which inhibits the beating and protein synthesis of cardiomyocytes. The inhibition in protein synthesis preceded the beating changes, and might be related to the deterioration of contractile function seen in menadione cardiotoxicity. A heat shock protein (HSP 70) was induced in cells exposing to 42°C for 60 min, but heat shock protein expression in culture cardiomyocytes can not be used as a tool to monitor cardiotoxicity of menadione.

1. INTRODUCTION

Menadione (2-methyl-1, 4-naphthoquinone, vitamin K_3) has been shown to inhibit the growth of tumor cells in vitro[1]. In the human tumor stem cell soft agar cloning assay, menadione causes inhibition of clonal growth of a wide variety of tumor cell types. Its anticancer activity with this assay is superior to currently used standard chemotherapeutic agents, such as adriamycin[2,3]. The mechanisms of the

effect of menadione on the growth inhibition of tumor cells in culture are obscure. Due to the same quinone structure as adriamycin, menadione may also exhibit cardiotoxicity. We are interested in cardiotoxic effects. Mammalian cardiomyocytes grown in culture maintain their ability to beat autorhythmically and thus can provide a simple in vitro system to study the effects of menadione on the structure and function of cardiomyocytes. We are attempting to establish the heat shock response in cardiomyocytes as a test system for early cardiac damage.

After being sumitted to a temperature stress, cells from bacteria to man synthesize a specific set of evolutionary conserved polypeptides: the heat shock proteins. Some of heat shock proteins are already made by non-stressed cells. Heat shock proteins were first described by Ritossa in Drosophila melanogaster[4,5] and have been proven to be a general cellular response to cell-damaging stress in many organisms and tissues of various origin.

As a model system we used primary cardiomyocytes culture prepared from neonatal rats. In the first part of our investigation we established the response of cardiomyocytes to heat shock, including the changes of beating rate and the formation of heat shock proteins. For model conditions we used temperature shock, which is known to induce heat shock proteins synthesis in other cellular system[6,7]. In the second part we looked for the effect of manadione, an anticancer drug, which was suspected to have cardiotoxic effects.

Our results indicate that menadione is cardiotoxic: it inhibited the beating and the protein synthesis ability of cardiomyocytes. The inhibition of protein synthesis preceded the beating changes of menadione cardiotoxicity. Heat shock of 1 hr at 42°C depressed the protein synthesis of cardiomyocytes and induced the synthesis of a heat shock protein. Heat shock proteins were not induced when cells exposed to menadione. Heat shock protein expression in cardiomyocytes can not used to monitor the cardiotoxicity of menadione.

2. MATERIALS AND METHODS

(1) Materials

^{35}S-methionine (specific activity$>$1,000 Ci/mmol) and films for autora-

diography were from Amersham. Menadione sodium bisulfate were from Sigma. Methionine-free DMEM, F10, horse serum and fetal bovine serum were obtain from Gibco. Anti-actin antibody and FITC-labeled goat anti-rabbit antibody were obtained from Bioyada. The gel drier was Bio-Rad, model 583. Fixer and developer were from Kodak. Cocktail, Omni-Szintisol, was from Merck. All other chemicals were of reagent grade.

(2) Culture of cardiomyocytes

Cardiomyocytes of neonatal Wistar rats (0-3 days) were prepared by a modified method of Lau et al.[8]. Cells were collected and washed with a medium composed of 80% (v/v) F10/10% (v/v) horse serum/10% (v/v) fetal bovine serum/14 mM $NaHCO_3$/20 mM Hepes, pH 7.4. To enrich cardiomyocytes in the cell preparation, the differential replating procedure of Blondel et al.[9] was followed. The cells were plated in a 100 mm Nauce dish and incubated in a 5% CO_2 incubator at 37°C for 3 h. For the various experiments the unattached cells were replated at different density. Cells were used within 2-3 days of preparation. After a 2-day culture, 90% of the cells were cardiomyocytes. The cell morphology was examined under a phase-contrast microscope. Cell degeneration was indicated by the distortion of cell morphology and was confirmed also by Trypan Blue-exclusion test[10].

(3) Morphology and beating observations

The morphology and beating of cardiomyocytes were observed under phase-contrast microscope equipped with temperature controlled air stage. Cells, which were beating regularly, were selected for each experiment. Beating of each cell was usually counted for 30 s.

(4) Immunofluorescence staining of actin filaments

Cardiomyocytes were distinguished from fibroblast by immunofluorescence staining of actin filaments. Cell grown on coverslips were washed three times with Tyrode solution[11], fixed with 3.5% formaldehyde in PBS (5 mM phosphate, 150 mM NaCl, pH 7.4) and permeabilized with 0.1% Triton X-100 in Tyrode solution. After washes, the cells were

incubated with rabbit anti-actin antibody, then washed with Tyrode solution. After washes, the cells were incubated with second antibody, FITC-labeled goat anti-rabbit IgG. After extensive washing, the cells on coverslips were mounted on microscopic slides in a drop of 50% glycerol in Tyrode solution. The cells were observed on a aus JENA fluorescence microscope. Fluorescence micrographys were recorded on Kodax Tri-X film.

(5) Labeling of the cells with ^{35}S-methionine

After incubation of the cells (5×10^5 cells/dish) for definite times with menadione or after heat shock, cells were labeled with 100 uCi ^{35}S-methionine in methionine-free DMEM supplemented with 5% fetal bovine serum for 3 h at 37°C in a water-saturated 5% CO_2 incubator. The labeling was stopped by removing the supernatant and the cells adhering to the dishes were washed with ice-cold PBS solution, and harvested with TEG solution (0.125% trypsin, 0.1% EDTA, 0.1% glucose). Cells were then washed with cold PBS, resuspended in Laemmli sample buffer[12] and frozen and thawed. Cell lysates were clarified in a Kubota microfuge, and either used directly or stored at −70°C. An aliquot of each supernatant was counted in a LKB-1219 Rack-beta liquid scintillation counter with Merck Omni-Szintisol cooktail for ^{35}S-methionine incorporation. Equal amount of radioactivities were applied to $NaDodSO_4$ polyacrylamide gel.

For the assay of the effect of heat shock or menadione on the protein synthesis, cells (5×10^4 cells/well of 4-well microplate) were incubated with menadione and 20 uCi ^{35}S-methionine in DMEM supplemented with 5% fetal bovine serum at 37°C for definite time or incubated with ^{35}S-methionine containing medium under various temperature. The reaction was stopped by removing the supernatant.

The cells were washed with cold PBS and lysed with PBS −1% Triton X-100. The cell lysates were clarified in a Kubota microfuge. TCA was added to supernantant to final concentration of 20% and placed in 4°C overnight. Acid-precipitable radioactivites were collected on glass fiber filters and washed with 20% TCA, ethanol, and ethyl ether for several times. Filters were then dried and radioactivities were

counted in a scintillation counter.

(6) NaDodSO$_4$ polyacrylamide gel electrophoresis

NaDodSO$_4$ polyacrylamide gel electrophoresis was done as described by Laemmli[12] except that the separating gel consisted of a 5-20% polyacrylamide gradient. The slab gel was run for 5 h at 150 V. Visualization of the proteins was done by either Coomassie blue staining or autoradiography.

(7) Autoradiography

After electrophoresis, the gels were dried with a gel-drier and exposed to Amersham hyper-film-β_{max} film for about 120 h. The films were developed and fixed in a commercial system supplied by Kodak.

3. RESULT

(1) Characteristics of cardiomyocytes

There are two kinds of cells in the cardiomyocytes primary culture: cardiomyocytes (Fig. 1) and fibroblasts (Fig. 2). Cardiomyocytes were distinguished by a granular cytoplasm with neumerous mitochondria. The nucleus of cardiomyocytes was small, round, and usually contained only one nucleolus, whereas the nucleus of fibroblast was larger, oval, and had two or more nucleoli. Cardiomyocytes were further certified by immunofluorescence staining of actin filaments. Figure 3 showed that actin filaments of cardiomyocytes were banded. In our cases, cardiomyocytes were 90% pure after 1-2 days in culture (average from 20 separate preparations), and remained more than 80% pure after 3-4 days in culture. Fibroblasts divided more rapidly than the cardiomyocytes, and accounted for a much highly percentage of the cell population than origin after several days in culture. In our experiments, only cells cultured 2-3 days were used.

For single cell cultures, the cells were plated at a density of 10^5 cells or less per petri dish (35 mm$\times$10 mm). Cells beat rhythmically and independently with 6-140 beats/min at 37°C. Most cells stopped beating at 21°C. When the cells were plated at higher density 2-4$\times10^5$ cells

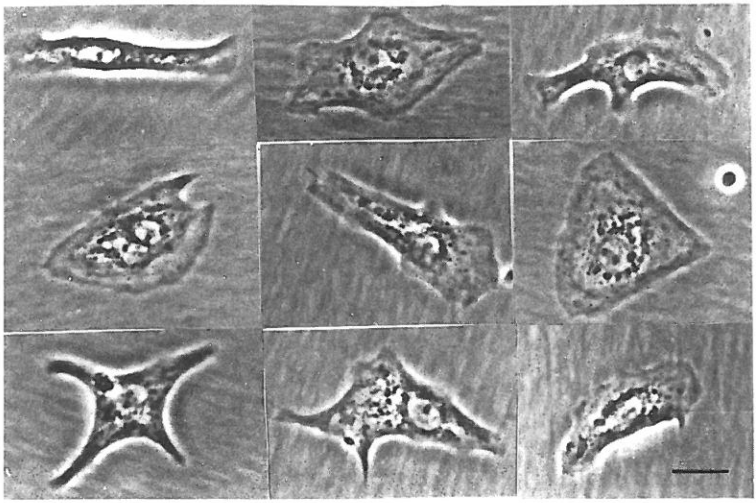

Fig. 1. Morphology of single cardiomyocytes under phase contrast microscope. Bar represents 10 μm.

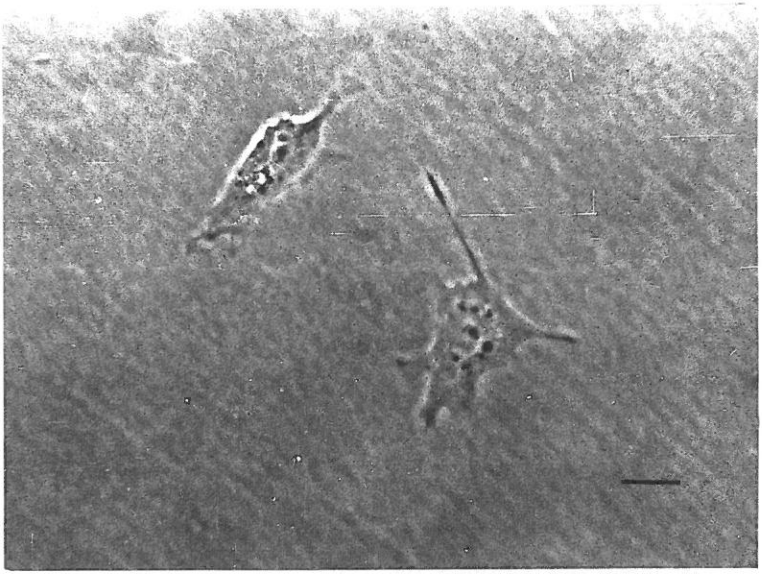

Fig. 2. Fibroblast morphology under phase contrast microscope. Note oval shape of nucleus containing more than one nucleoli. Bar represents 10 μm.

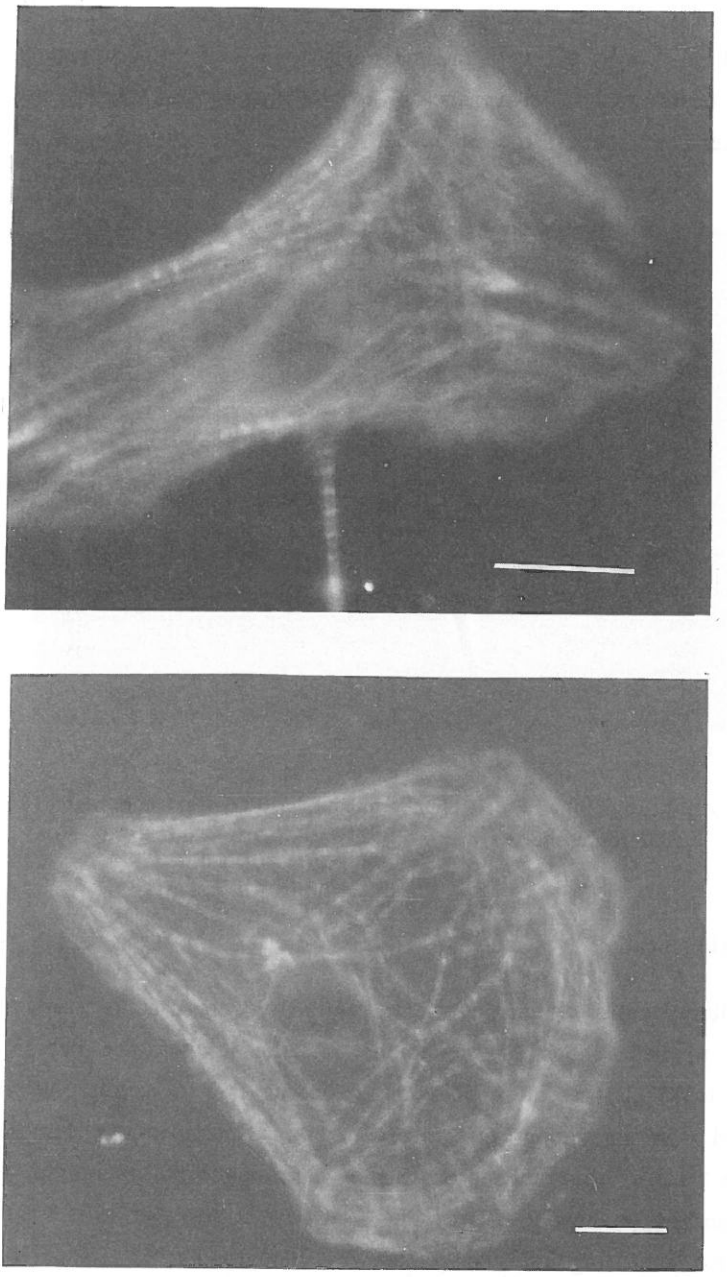

Fig. 3. Actin filaments distribution of cardiomyocytes under fluorescence microscope. Bar represents 10 μm.

per dish, cells became contact with each other forming a large cell clusters (Fig. 4). All the cells in a given cell cluster beat synchronously at 21-200 beats/min. The average of the cell clusters was more stronger and quicker than that of the single cells.

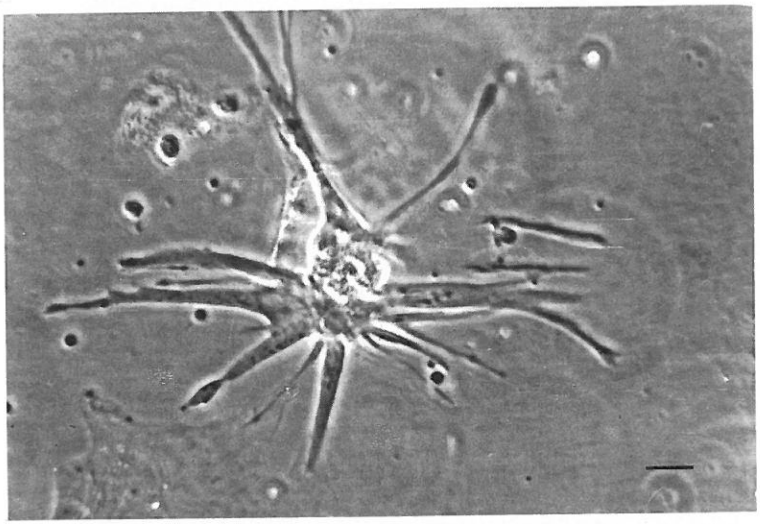

Fig. 4. Morphology of cell cluster under phase contrast microscope. Bar represents 10 μm.

(2) Beating study

Cardiomyocytes, which contracted regularly, were used to study the response to heat shock or menadione. As the temperature decreased from 37 to 30°C, the rates of spontaneous beating of cardiomyocytes decreased. As the temperature increased from 37°C to higher temperature, the rates of spontaneous beating of cardiomyocytes increased, and the higher the temperature, the higher the beating rates of cells (Fig. 5). Although the beating rates of cells was changed as the temperature varied, the beating of cells was still regular. The morphology of cells did not change even at temperature as high as 50°C.

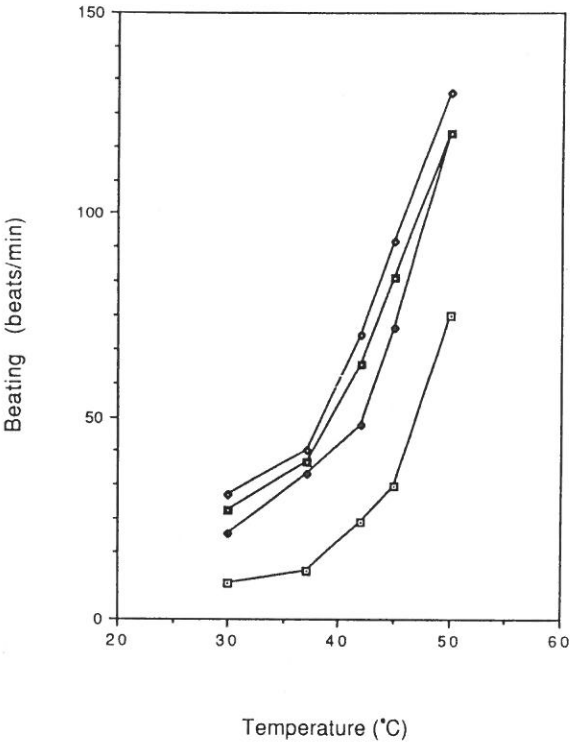

Fig. 5. Effect of temperature on the rates of beating of cardiomyocytes. Beating of cardiomyocytes were observed under phase-contrast microscope equipped with temperature controlled air stage. Cells, which were beating regularly, were selected for experiment. Beating of each cell was usually counted for 30 s. The curves in the figure represent the response of four cells.

Beating status of cardiomyocytes is a sensitive and reliable parameter in cardiomyocytes culture system for studies on the cardiotoxicity of drugs. Figure 6 shows the results of treatment with menadione. Addition of menadione inhibited the beating of cells. The inhibition by menadione was dose and time-dependent. Cultures exposed continuously to 20 uM menadione no longer beat after 80 min. At higher menadione doses (80 uM), cells stopped beating within 30 min of exposure. Despite individual variations in the timing of the changes, the changes observed in each cell seemed to possess similar features. Initially, the beating

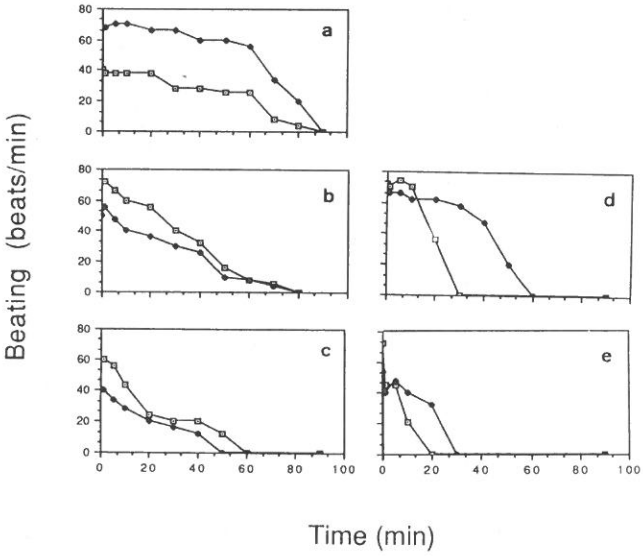

Fig. 6. Effect of menadione on the rates of beating of cardiomyocytes. Beating of cardiomyocytes were observed under phase-contrast microscope at 37°C. Cells, which were beating regularly, were selected for experiment. Beating of each cell was usually countd for 30 s. Menadione concentration: (a) 10 μM, (b) 20 μM, (c) 30 μM, (d) 40 μM, (e) 80 μM. The curves in each plot represent the response of two cells.

rate of cells became slow and stopped finally. The cells fibrillated quickly before beating stopped. Even as the beating of cells was stopped, the cells still remained alive. Continued treatment of cells resulted in the death of the cells.

(3) Protein synthesis

Protein synthesis was analyzed in cardiomyocytes during incubating with menadione or under various heat shock condition. The cardiac response was estimated using the amount of ^{35}S-methionine incorporated into proteins in cardiomyocytes. Protein synthesis of cells was not significantly altered by less than 30 min shift from 37 to 42°C but falled sharply after a shift to 42°C for 1 hr. A 1-hr incubation at 42°C resulted in 37% depression of protein synthesis. In the case of mena-

dione, the levels of protein synthesis were decreased as cardiomyocytes were incubated with menadione. The inhibition by menadione was dose and time-dependent (Fig. 7). After 10 min of treatment with 20 uM and 40 uM menadione, protein synthesis was inhibited by 64% and 82%, respectively. After 60 min of treatment with 20 uM menadione, protein synthesis was almost completely inhibited.

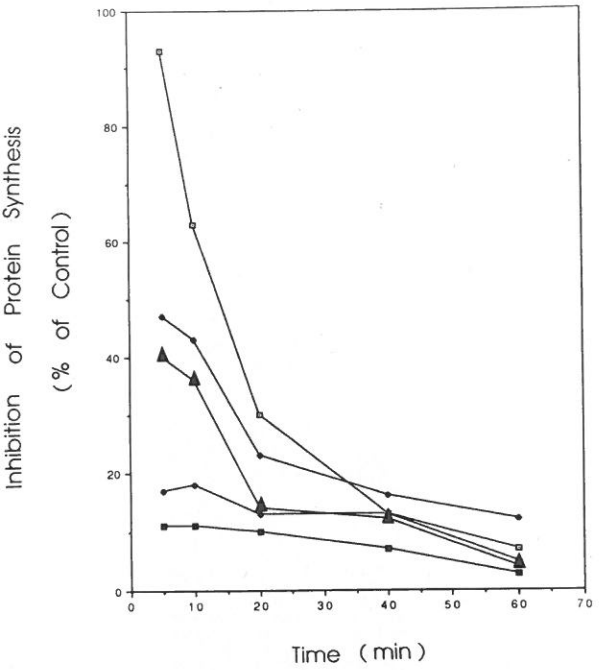

Fig. 7. Inhibition effect of menadione on protein synthesis of cardiomyocytes. Cardiomyocytes were incubated with menadione in ^{35}S-Methionine containing medium for various time. The TCA-precipitable fraction was collected and counted with β-counter. Symbols: □, 5 μM; ◆, 10 μM; ▲, 20 μM; ◇, 40 μM; ■, 80 μM.

(4) Heat shock protein induction

Based on the results above, 5 and 20 uM concentrations of menadione were chosen to examine effects on heat shock protein induction. The

proteins of cardiomyocytes separated on $NaDodSO_4$ polyacrylamide gel electrophoresis presented in Fig. 8. The polypeptide pattern did not change significantly from preparation to preparation. As shown in Fig. 8B, exposure of the cardiomyocytes to heat, 42°C for 60 min, induced

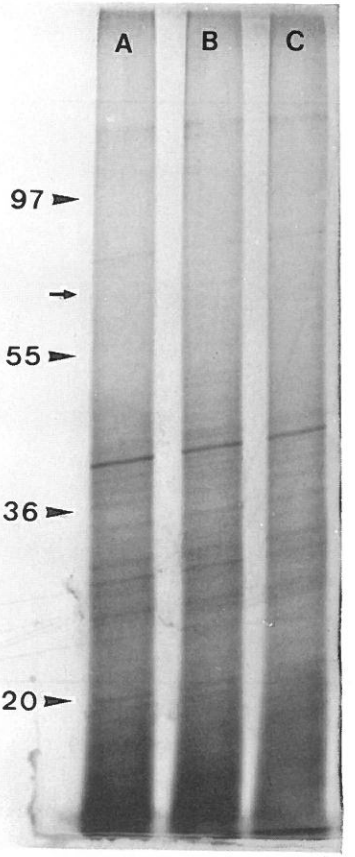

Fig. 8. Three-day-old cardiomyocytes: (a) incubated at 37°C for 60 min. (b) incubated at 42°C for 60 min. (c) incubated with 5 uM menadione for 10 min. Thereafter 80 uCi of ^{35}S-methionine was added. The cells were kept for a further 3 h at 37°C. Then the supernatant was discarded and the washed cells were collected and lysed in electrophoresis sample buffer. 100,000 cpm was applied per slot to $NaDodSO_4$-polyacrylamide gradient (5-20%) gel electrophoresis. Arrow indicates position of a heat shock protein of Mr 70 kD.

the de novo synthesis of a heat shock protein (MW 70,000). Exposure of the cells to 42°C for less than 30 min did not induce any new proteins synthesis. Exposure to 5 uM menadione for 10 min did not induce any new protein synthesis (Fig. 8C). Exposure to 1 or 20 uM menadione for 20 or 10 min also did not induce any new protein synthesis (data not shown).

4. DISCUSSION

The heat shock response is now known to be a rapid and transient reprogramming of cellular activities that ensures survival during the stress period, protects essential cell components against damage, and permits a rapid resumption of normal cellular activities during the recovery period. Stress can be extered in the form of toxic substances, e. g. cadmium chloride, H_2O_2, or heat. Hence we are mointor temperature shock and chemical stress of menadione in cardiomyocytes.

The response of cardiomyocytes to temperature shock involved a depression in the synthesis of most proteins normally made at 37°C and a increase in the relative rate of synthesis of a protein with M. W. 70,000 (HSP 70). The synthesis of HSP 70 is temperature-dependent. It is detectable after 1 hr at a incubation temperature of 42°C. In the myocardium, the synthesis of HSP 70, the most highly conserved stress protein, has been described after various traumas such as hypoxia, ischemia and heat shock[13]. Low reported that heat shock protein expression in cardiomyocytes is a useful model system to monitor cardiotoxicity of chemical agents[14] and heat shocks induced the synthesis of two proteins of 71 and 68 kD. In our cases, heat shock (42°C, 60 min) only induces a heat shock protein synthesis (HSP 70). While heat shock responses had been investigated since 1962, the function of these proteins were still unclear. It needs further study to certify the role of HSP 70.

There are many reports suggest that the antitumor activity of menadione is superior to adriamycin. Due to the quinone structure, menadione may exhibit cardiotoxicity. In this study, we have shown that menadione is cardiotoxic. It inhibited the beating of cardiomyocytes in a time and concentration dependent manner and even killed the cells

at higher dosage or with longer incubation time (Fig. 6).

It emeraged from this study that inhibition in protein synthesis was associated with the response of cardiomyocytes to menadione. The inhibition was very obvious (Fig. 7) and preceded the beating changes of menadione cardiotoxicity: treatment of cells with 10 uM menadione for 10 min inhibited the protein synthesis by 57%, but it did not significantly inhibited the beating of the cells. It emerged from this study that alternations in protein synthesis were associated with the early response of cardiomyocytes to menadione. Whether the inhibition of protein synthesis by menadione is specific or nonspecific? It is possible that the cessation of beating may be reflecting the inhibition of protein synthesis. It needs further investigation. While protein synthesis was inhibited as cells incubated with menadione, heat shock proteins were not induced under the same condition.

In summary, Heat shock protein of 70 kD was induced in response to heat shock (42°C for 60 min) in cardiomyocytes. Menadione has cardiotoxic effects. It inhibits the protein synthessis and beating of cardiomyocytes in a time and concentration dependent manner, although heat shock proteins had not been induced in the cells. From our results, heat shock proteins synthesis can not serve as a sensitive system to monitor the cardiotoxicity of menadione.

REFERENCES

(1) K.N. Prasad, J. Edwards-Prasad and A. Sakamoto, *Life Sci.*, **29**, 1387 (1981).
(2) S.A. Akman, M. Dietrich, R. Chlebowski, P. Limberg and J.B. Block, *Cancer Res.*, **45**, 5257 (1985).
(3) E. Cortes, G. Lutman, J. Wanka, J. Picken, J. Wallace and J. Holland, *Cancer Chemother. Rep.*, **6**, 215 (1975).
(4) F. Ritossa, *Experimentia*, **18**, 571 (1962).
(5) F. Ritossa, *Exp. Cell Res.*, **35**, 601 (1964).
(6) D.R. Spitz, W.C. Dewey and G.C. Li, *J. Cell Physiol.*, **131**, 364 (1987).
(7) M. Pouchelet, E. St-Pierre, V. Bibor-Hardy and R. Simard, *Exp. Cell Res.*, **149**, 451 (1983).
(8) Y.H. Lau, R.B. Robinson, M.R. Rosen and J.P. Bilezikian, *Circ. Res.*, **47**, 41048 (1980).
(9) B. Blondel, I. Roijen and J.P. Cheneval, *Experimentia*, **27**, 356 (1971).
(10) M.R. Glick, A.H. Burns and W.J. Reddy, *Anal. Biochem.*, **60**, 32 (1974).

(11) H.M. Piper, P. Schwartz, J.F. Hutter and P.G. Spiecker, *J. Mol. Cell. Cardiol.*, **16**, 995 (1984).
(12) U.K. Laemmli, *Nature*, **227**, 680 (1970).
(13) C. Delcayre, J.L. Samuel, M. Best-Belpomme, J.J. Mercardier and L. Rappaport, *J. Clin. Invest.*, **82**, 460 (1988).
(14) I. Low, T. Friedrich and W. Schoeppe, *Exp. Cell Res.*, **180**, 451 (1989).

Menadione 對新生大白鼠心臟細胞之毒性研究

曾婉芳　黃仁奕

輔仁大學生物系

摘　要

本實驗乃以新生大白鼠心臟細胞研究抗癌藥物 menadione 之心臟毒性。Menadione 隨劑量及作用時間增加明顯的抑制心臟細胞的跳動。在 80 μM 濃度下，心臟細胞的跳動在 30 分鐘內就完全停止了。時間加長，則導致細胞死亡。在心臟細胞培養液中加入放射性的 ^{35}S-methionine 測試 menadione 或熱處理 (heat shock) 對細胞蛋白質合成及熱休克蛋白質引發的影響。結果發現 menadione 會抑制蛋白質的合成。細胞在 42°C，1 小時，其蛋白質合成受到抑制，且引發一熱休克蛋白 HSP-70 的合成。但 menadione 卻無法引發熱休克蛋白的合成。

本實驗結果顯示 menadione 具心臟毒性，其抑制心臟細胞之跳動及蛋白質合成，而蛋白質合成受抑制的發生時間早於細胞跳動受抑制的時間，故蛋白質合成之抑制可能和 menadione 引發之心臟有關。心臟細胞在 42°C，1 小時，會引發一熱休克蛋白，但熱休克蛋白的表現卻無法作爲測試 menadione 心臟毒性的指標。

本省日用食品鋁含量之初步調查

王果行　吳瑞芸

輔仁大學理工學院食品營養系暨研究所

摘　要

鋁的毒性在最近一、二十年較受到人們注目，飲食中鋁的來源可由自然食物，食品添加物，鋁製烹飪用具或含鋁的藥劑而來，本實驗挑選數種常用的食物，經溼式分解後，由原子吸光分析儀測定其中鋁的含量。結果顯示，肉製品中以蝦及牡蠣含鋁量較高，分別爲 13.54±0.48 及 10.12±0.03 μg/g，其他豬、牛、鷄、魚肉及加工肉類之平均含鋁量由 <0.21 至 5.35 μg/g 不等。而豆蛋類中皮蛋較鹹鴨蛋有較高的鋁含量。蔬菜類中以海帶含鋁量最高 (699.21±69.12 μg/g)，蕃茄、青椒、高麗菜等最低（皆 <0.50 μg/g)。水果類中鳳梨、芭樂、芒果、荔枝含鋁量較低（平均皆 <0.46 μg/g)，青蘋果的含鋁量較大 (6.98±0.75 μg/g)。五穀類中，清蛋糕可能由於添加含鋁的膨脹劑，含鋁量較高，達 82.72±15.70 μg/g。其他點心類中草莓夾心及蝦味先較高，含鋁量達 20～30 μg/g 之間。飲料中似乎鋁罐裝檸檬茶有較高的含鋁量，大約在 2.5 μg/ml 左右。

一、前　言

鋁在地殼中含量豐富，而且普遍存在於我們日常生活中，空氣中有鋁，自然食物中，烹調時所用的鋁鍋，鋁盤、鋁箔紙等、淨化水質所用的明礬，醫療用的制酸劑，甚至合法的食品添加物[1,2] 皆含有鋁。根據近年來的臨床報告指出：鋁可能是引起慢性腎衰竭洗腎病人產生洗腎性骨骼病變（Dialysis osteomalacia）及洗腎性腦病變 (Dialysis encephalopathy) 的原因[3~7]。從這些病人的組織切片圖顯示：在骨骼組織中有大量鋁的沈積，影響骨質礦化 (Mineralization)，而使得骨質流失[3,4,7]。在病患腦部的海馬區 (Hippocampus) 內有高濃度的鋁，可能導致該處神經細胞纖維老化且互相糾結[3,5]。推究其因，可能是因腎衰竭病人長期使用含鋁量高的透析液及口服含鋁的制磷劑 (Aluminum-containing phosphate binders) 所致，由於沒有正常腎功能調節，大量鋁離子堆積於體內而造成組織病變。另外，阿茲海默症 (Alzheimer's disease) 患者的腦部亦有較高的鋁含量[8,9]，而被提出鋁與阿茲海默症有某些關連存在。

因此，是否長期由飲食中攝取較高的鋁，也會對人體健康有所影響？以及鋁在一般飲食中的來源和含量，也引起了較廣泛的注意。本實驗的目的便是就常用的食品加以分析其中的鋁含量，希望能提供一些基本的資料。

二、材料與方法

1. 取樣

本實驗之取樣是於輔大附近傳統市場及臺北市東區超級市場隨機購買食物及飲料樣品共六十七種，如下列：

(1) 肉製品：豬肉（前腿肉），牛肉（絞肉），魚肉（大頭鰱），洋火腿（王記牌）等共九種皆購自臺北市東區超市。
(2) 豆蛋類：五香豆干等共四種皆購自新莊區傳統市場。
(3) 蔬菜類：除木耳及海帶購自新莊區傳統市場外，其他皆購自臺北東區兩家超市，共計十四種。
(4) 水果類：柳丁，青蘋果，鳳梨等十一種水果，皆購自新莊區傳統超市。
(5) 五穀類：共五種，白米（億東牌三好米）購自臺北東區超市，清蛋糕購自輔大附近之傳統式麵包店，甜不辣則採購於傳統市場。
(6) 點心類與飲料類：點心類六種及飲料十六種皆購自輔大附近小型商店。

2. 樣品前處理

水份含量較高的樣品如蔬菜，水果，肉製品等皆先稱取適量之可食部分，置於 110°C 烘箱，24小時，除去部分水份後，加入適量的濃硫酸及濃硝酸，加熱分解至澄清。數種較濃稠的飲料如果汁，牛奶等及水份含量較低的食物如豆蛋類，五穀類，於稱取樣品後直接加酸分解。所有的樣品皆做二重覆分析。分解液定容後，存放於塑膠管中，加蓋密封，留待原子吸光分析儀測定鋁含量。

3. 鋁之測定

樣品分解液中鋁含量乃採用原子吸光分析儀 (Z-8000，Polarized Zeeman Atomic Absorption Spectrophotometer，Hitachi)，裝置 Hollow-cathode 鋁燈管及高溫燃燒頭，以笑氣 (N_2O)-乙炔 (C_2H_2) 爲燃料，雙光束及背景校正等條件下測定吸光值。並配製 1、5、10、20 μg/ml 不同濃度的標準溶液完成校正曲線 (Calibration curve)，以此爲基準計算出樣品中鋁之濃度。

爲了解樣品前處理過程的可信度，取數種濃度的鋁標準液，經上述濕式分解後，亦測定其中鋁含量，求得回收率。

三、結果與討論

由濕式分解鋁標準溶液 5～50 μg/ml 的回收率爲 91.1 至 106.9%不等，平均回收率爲 101.8±4.8%（表一）。

表一 鋁之標準液經濕式分解後之回收率

初始濃度 (μg/ml)	最後濃度 (μg/ml)	回收率[1] (%)
5	5.35	106.9±4.60
10	10.48	104.7±0.07
20	20.12	100.6±0.00
50	45.56	91.1±0.98

[1] Mean±S.E. of 2 replicates.

結果顯示肉製品中鋁含量由豬肉的平均0.21 μg/g到含量最高的蝦13.54 μg/g不等（表二）。豆蛋類中皮蛋含鋁最高達 12.91 μg/g。水果類大部份樣品皆低於2 ppm，僅青蘋果含鋁量最高達 6.98 μg/g。蔬菜類含鋁量因種類差異很大，由最低的青椒 0.37 μg/g 到海帶 699.21 μg/g。五穀類中不同食品含鋁量的差異也很大，由最高的清蛋糕 82.72 μg/g 到最低的白米，白土司小於 2 μg/g。點心類中鋁含量由最高達約 30 μg/g 的草莓夾心到 <2.40 μg/g 的旺旺仙貝。所有的飲料鋁濃度皆小於 3 μg/g，八種鋁罐裝飲料有七種鋁含量超過 1 μg/ml。含量最高者爲鋁罐裝檸檬茶，平均鋁含量超過了 2 μg/ml（表三）。如果飲用一罐其中含鋁量最高的檸檬茶，約攝取 1 mg 的鋁。

生物體中鋁的含量會受到生長環境的土壤及水源中含鋁量，酸鹼度等因素所影響。一般而言，自然植物體中含鋁量較動物體來得高[2]，主要原因可能是動物攝食植物又經過消化吸收的過程，而一般認爲動物體對鋁的吸收率很低。肉類中鋁的含量則可能與動物本身所吃的飼料或牧草中含鋁的多寡有關[10]。本實驗之生鮮食品皆由市場中購得，不單是這些食品之原產地不可得知，即使知道原產地，當地土壤、水質含鋁的資料亦缺如，故單就動植物食品之差別，來分類比較，將會十分混淆。

食物中鋁的含量還受到是否加入含鋁的食品添加物及加工過程所影響。調查報告指出，1970年及1982年美國人每人每日平均由食品添加物（例如：發泡劑、乳化劑等）所攝取的鋁，分別是 18.7 及 21.5 mg[2]。而加工食品中 Processed cheese（含鋁量 0.297 μg/g）與 Natural cheese（含鋁量 0.015 μg/g）中鋁含量約有20倍的差距。中華民國行政院衞生署於民國七十七年出版的「食品添加物使用範圍及用量標準」[1] 即指出合法的含鋁食品添加物包括了膨脹劑（如：鉀明礬，鈉明礬等），乳化劑（如 Sodium aluminum phosphate basic 等數種），品質改良用，釀造用及食品製造用劑（如：硫酸鋁，矽酸鋁等），另外還有着色劑（如：食用紅色七號鋁麗基、食用綠色三號鋁麗基等）。這些含鋁的食品添加物皆常用於加工食品中。本實驗由於樣品種類及數量的限制，雖無法在統計上做

表二 各種食物中的鋁含量[1)]

種類	鋁含量 (μg/g)	種類	鋁含量 (μg/g)
肉製品：		蔬菜類：	
豬肉	0.21±0.06	空心菜	3.45± 0.84
牛肉	<0.50±0.00	高麗菜	0.38± 0.01
魚肉	0.47±0.01	芥藍菜	3.85± 0.14
鷄肉	1.91±0.28	青剛菜	3.04± 0.03
蝦	13.54±0.48	大白菜	2.18± 0.11
牡蠣	10.12±0.03	蕃茄[2)]	<0.48± 0.00
魷魚絲	4.15±0.16	青椒	0.37± 0.03
洋火腿	0.30±0.02	洋葱	9.03± 0.31
肉鬆	5.35±0.13	胡蘿蔔[2)]	4.72± 0.31
豆蛋類：		冬筍	10.41± 0.08
五香豆干	6.59±0.94	木耳	6.66± 0.44
鹹鴨蛋	5.26±1.47	濕香菇	19.35± 0.19
皮蛋	12.91±0.48	毛豆仁	4.36± 0.05
土皮蛋	12.06±3.45	海帶	699.21±69.12
水果類：		五穀類：	
柳丁	1.39±0.39	白米[4)]	1.10± 0.10
橘子	1.21±0.05	白土司	1.79± 0.94
青蘋果[2)]	6.98±0.75	清蛋糕	82.72±15.70
荔枝	<0.45±0.01	甜不辣（長）	23.45± 4.04
芒果	<0.46±0.02	甜不辣（圓扁）	39.82± 1.08
芭樂[2)]	0.33±0.04	點心類：	
鳳梨	0.08±0.00	蝦味先	23.60± 2.32
香蕉	0.91±0.03	旺旺仙貝	<2.40± 0.13
蓮霧	1.29±0.02	金牛角玉米點心	<2.79± 0.03
香瓜[3)]	0.48±0.04	波卡洋玉片	<2.46± 0.07
西瓜	0.41±0.12	可口可喜	5.55± 1.29
		草莓夾心	29.20± 2.01

1) Values are Mean±S.E.。
2) 連皮。
3) 去皮。
4) 乾燥米粒。

出有意義的結論，但若以前人之報導來比較，似可略窺一斑。肉製品中，加工食品（如：肉鬆），似乎較新鮮豬肉有較高的鋁含量。皮蛋較同類食品（鹹鴨蛋）含較高濃度的鋁，可能是由於包蛋的土（土皮蛋）或浸蛋的溶液（一般皮蛋）中

表三 各種飲料中的鋁含量

種類	鋁含量[3]		pH 值	包裝材料
	(μg/ml)	(μg/box)		
味全鮮果汁[1]	0.41±0.06	97±14	3.34	紙盒
光泉芭樂汁[1]	0.13±0.00	26±0	3.96	利樂包
光泉水蜜桃汁[1]	1.07±0.10	214±20	3.70	利樂包
統一楊桃汁[2]	1.74±0.04	348±8	3.11	鋁箔包
統一麥芽豆奶[1]	0.30±0.03	60±6	6.39	鋁箔包
統一鮮奶[1]	0.41±0.06	97±14	6.69	紙盒
光泉保久奶[1]	0.50±0.06	100±12	6.66	鋁箔包
光泉鮮奶[1]	0.25±0.03	59±7	6.69	利樂包
維大力汽水[2]	0.74±0.02	263±7	3.37	鋁罐
雪士達櫻桃汽水[2]	1.57±0.09	557±32	2.91	鋁罐
台鳳鳳梨汽水[2]	1.22±0.18	433±64	3.49	鋁罐
蘋果西打[2]	1.01±0.11	359±39	3.43	鋁罐
麥根沙士[2]	1.25±0.04	444±14	3.30	鋁罐
金帝檸檬茶[2]	2.32±0.06	824±21	3.42	鋁罐
台鳳檸檬茶[2]	2.78±0.04	987±14	3.96	鋁罐
臺灣啤酒[2]	1.21±0.21	430±75	4.35	鋁罐

[1] 經濕式分解後測定。
[2] 不經濕式分解樣品直接以 A.A.S. 測定。
[3] Mean±S.E.

含較多的鋁，或者酸鹼度較適合鋁溶解，而使得較多的鋁經蛋殼浸入。值得注意的是海帶中鋁含量居全部樣品之冠，是否是海帶生長之海域含鋁量很高，或是發泡乾海帶時，使用了任何含鋁藥劑，則不可知。清蛋糕中含有很高量的鋁，可能由於製作過程中使用了含鋁的膨脹劑（如：Baking powder）而來。而加工過程繁複，且可能有較多食品添加物的甜不辣，亦較同類的白米，白麵包的含鋁量高二、三十倍。

另外，鋁製烹調器皿，也可能是飲食中鋁的來源之一。研究報告顯示[11]，以不同酸鹼度的食物，放入未經特別處理的鋁鍋中烹煮的結果，酸鹼性較強的食物比中性環境下溶出器皿的鋁高出百倍。而烹煮時間愈長，溶出的鋁愈多。因此就一加工食品而言，其鋁含量的來源，可能受到原料，加工處理（如：水質，器皿，添加物，處理條件等）及包裝材質等多項因素影響。本實驗之飲料部份，檸檬茶具備高酸度、原料茶含較高的鋁[2]，鋁製容器等數種因素，其含鋁量在飲料中居冠，似乎亦可預期。雖然一般鋁箔包的材料之內尚有一層塑膠薄膜，而由鋁

箔包的三個樣品中，楊桃汁的 pH 值達 3.11，鋁含量比其他二者（pH 約 6.5 左右）爲高的結果看來，可能此層薄膜亦有某種程度的通透性，致使鋁箔層的鋁因酸度高而溶於果汁中，但是楊桃汁原有原料中卽含有較高量鋁的此一因素亦不可排除。

實驗報告指出，若以美國成人爲例，每日由飲食中攝取的鋁約爲 7～50 mg，其中約20～25 mg 由食品添加物而來，由鋁製烹飪用具而來的鋁約爲3.5 mg[2]。比較本實驗飲料中含鋁最高的鋁罐裝檸檬茶(987 μg/罐），若於夏日每日飲用兩罐，則由此來源的鋁不超過 2 mg。值得注意的是許多不需處方的含鋁藥劑（例如：制酸劑），每日由藥劑攝取的鋁可較飲食中獲得的鋁高出 20～200倍 之多。

總之，應更有系統將食物分類，樣品種類數增加，同種食物樣品數目增加，並考慮樣品的地區性，季節性，採樣之代表性等因素，才能更完整的建立臺灣區食品鋁含量的基礎資料，進而以此做爲分析、了解國人攝食鋁量的基礎。

四、誌　　謝

本研究之完成承輔仁大學理工學院聖言會七十六學年度經費補助，統一公司臺北研究中心原子吸光分析儀的借用，謹此致最高的謝意。

參 考 文 獻

(1) 行政院衞生署，食品添加物使用範圍及用量標準，食品衞生管理手册之二，20 頁 (1988)。
(2) J.L. Greger, "Aluminum Content of the American Diet", *Food Techol.*, **5**, 73 (1985).
(3) A.C. Alfrey, A. Hegg and P. Craswell, "Metabolism and Toxicity of Aluminum in Renal Failure", *Am. J. Clin. Nutr.*, **33**, 1509 (1980).
(4) H.G. Nebeker and J.W. Coburn, "Aluminum and Renal Osteodestrophy", *Ann. Rev. Med.*, **37**, 79 (1986).
(5) A.C. Alfrey, G.R. LeGendre and W.D. Kaehny, "The Dialysis Encephalopathy Syndrome: Possible Aluminum Intoxication", *N. Engl. J. Med.*, **294**, 184 (1976).
(6) L. Finberg, H.S. Dweck and F. Holmes, "Aluminum Toxicity in Infants and Children", *Pediatr.*, **78**, 1150 (1986).
(7) F.L. VandeVyver and M.E. DeBroe, "Aluminum in Tissue", *Clin. Nephrol.*, **24**, 84 (1985).
(8) D.R. Crapper, S.S. Krishnan and A.J. Dalton, "Brain Aluminum Distribution in Alzheimer's Disease and Experimental Neurofibrillary Degeneration", *Science*, **180**(4), 511 (1973).
(9) D.P. Perl and A.R. Brody, "Alzheimer's Disease: X-Ray Spectrometric

Evidence of Aluminum Accumulation in Neurofibrillary Tangle-Bearing Neurons", *Science*, **208**(18), 297 (1980).
(10) S.J. Fairweather-Tait, R.M. Faulks, S.J.A. Fatemi and F.R. Moore, "Aluminum in the Diet", *Human Nutr., Food Sci. and Nutr.*, **41**, 183 (1987).
(11) T. Inoue, H. Ishiwata and K. Yoshihira, "Aluminum Levels in Food-Simulating Solvents and Various Foods Cooked in Aluminum Pans", *J. Agric. Food Chem.*, **36**, 599 (1988).

Aluminum Content of Foods in Taiwan—Report I

GUOO-SHYNG WANG HSU AND JUI-YUN WU
Department of Nutrition and Food Sciences

ABSTRACT

Aluminum toxicity has been obtained great concern during last two decades. Dietary sources of aluminum included from natural foods, food additives, aluminum cooking utensils, and aluminum-containing medicines. In this study, 67 foods and beverages were selected to determine the aluminum content by Atomic Absorption Spectrophotometry after acid digestion. Results indicated that shrimp and oyster had the highest Al values among meat products, containing 13.54 ± 0.48 and 10.12 ± 0.03 μg/g Al, respectively. Aluminum concentrations in other meat products ranged from <0.21 to 5.35 μg/g. Thousand-year eggs had higher Al content than salty duck eggs did. In vegetable group, kelp had 699.21 ± 69.12 μg/g Al, and tomatoe, green pepper and cabbage had <0.50 μg/g Al. The lowest value (avarage <0.46 μg/g Al) in fruits was found in pineapple, guava, mango and litchi. Green apple had 6.98 ± 0.75 μg/g Al. In grain-cereals group, angel-food cake had the highest Al, i.e. 82.72 ± 15.70 μg/g. The highest Al content in cookies and snacks was 20 to 30 μg/g. Lemon tea with aluminum canteen had the highest Al value (around 2.5 μg/ml) among beverages.

ABSTRACTS OF PAPERS BY FACULTY OF THE COLLEGE OF SCIENCE AND ENGINEERING THAT APPEARED IN OTHER REFEREED JOURNALS DURING THE 1989 ACADEMIC YEAR

Sers of Crystal Violet in Sandblast Roughened Silver Surface

PING PENG, KOW-JE LING (凌國基) AND W. S. TSE

Modern Physics Letters B, 4(8), 531-534 (1990)

In this paper we present an alternative way for SERS-active substrate preparation, the sandblast method. The roughened surface prepared by this method is more durable than the silver coated surface which is easily spoiled by moisture. Because the roughness is almost only dependent on the size and the speed of the abrasive, the roughness of the surface can casily be controlled. The abrasives used were 100 μm Al_2O_3, 52 μm Garnet, 18 μm Garnet, and also 5 μm Garnet. Comparison between the sandblasted and unblasted substrates shows an enhancement factor of $\sim 10^3$. To our knowledge this is first paper about the SERS-active substrate prepared by this method.

Anomalous X-ray Atomic Scattering Factor for Zr, Nb, and Mo

M. S. WANG AND SHEAU-HUEY CHIA (賈小慧)

Physical Review A, 40(9), 5420-5421 (1989)

The anomalous x-ray atomic scattering factors for Zr, Nb, and Mo within ± 3 keV of the elements' K-absorption edge are calculated using both the Dirac-Slater and the Dirac-Kohn-Sham potentials. Both theories agree at the 1-2% level. However, significant systematic differences between theory and experiment are observed.

New Metal-Clad Fiber Polarizer

S. C. LEE AND JEN-I CHEN (陳振益)

Applied Optics, **29**(18), 2667-2668 (1990)

High quality fiber polarizers are made easily by consecutively overcoating suitably polished fibers with MgF_2 and Al films.

Reduction of Nonstationarity and Parameter Analysis of VHF Radar Returns from the Atmosphere

FU-SHONG KUO, HSIOU-YUNG LEU (呂秀鏞) AND SHU-ING LIU

Radio Science, **25**(4), 517-526 (1990)

An optimization process to reduce nonstationarity problem yet preserve the reliability of the radar echo signal distribution is developed combining the conventional χ^2 test and numerical simulation techniques. As an application to the real data, we determine the optimized data length to be 128 elements per set for SOUSY data and 256 elements per set for Chung-Li data. For each of such data sets, the echo power P and the modified Rice parameter γ are calculated and their statistics are examined. When their time average are plotted as functions of height, we frequently observe the existence of maximum P along with minimum γ in Chung-Li data. Such an coupling can be explained as an evidence of the existence of turbulence layer. The cause of the occurrence of turbulence layers in the troposphere over Chung-Li area is briefly discussed.

A General Preparation of 2-Acyl-3-(phenylthio)-1, 3-butadiences

SHANG-SHING P. CHOU (周善行), DER-JEN SUN AND SHIOW-JYI WEH

Synth. Commun., **19**, 1593-1602 (1989)

The title dienes **1** are prepared by thermolysis of 3-sulfolenes **2**, which are readily obtained by ultrasound promoted allylzincation of bromides **4** with aldehydes followed by PCC oxidation.

Spirodialkylation of 3-(Phenylthio)-3-sulfolene and Subsequent Synthetic Transformations

SHANG-SHING P. CHOU (周善行) AND CHIN-CHUAN SUNG

J. Chin. Chem. Soc., **36**, 601-607 (1989)

3-(Phenylthio)-3-sulfolene (**1**) underwent spirodialkylation to give products **2** which were desulfonylated to afford the dienes **3**. The Diels-Alder reaction of **3** was achieved for some reactive dienophiles to yield spiro compounds. Compounds **2** were alson converted to sulfonyldienes **9** which reacted as Michael acceptors.

A Facile Synthesis of Stable Precursors to 2-Alkylated and 2, 3-Dialkylated 1, 3-Butadienes

SHANG-SHING P. CHOU (周善行) AND CHUNG-MING SUN

Tetrahedron Lett., **31**, 1035-1038 (1990)

3-Sulfolenes **3**, stable precursors to 2-alkylated and 2, 3-dialkylated 1, 3-butadienes, were prepared in good yield from (**1**) by regiospecific alkylation and reductive desulfurization.

Intramolecular Diels-Alder Reactions of Sulfur-Substituted Dienes via 3-Sulfolenes

SHANG-SHING P. CHOU (周善行) AND SHIOW-JYI WEY

J. Org. Chem., **55**, 1270-1274 (1990)

Sulfur-substituted dienes containing an unsaturated alkyl chain were readily prepared from 3-sulfolenes. The intramolecular Diels-Alder (IMDA) reaction of these derivatives was studied for the first time. A sulfonyl group on the diene was found to facilitate the IMDA reaction. Hexahydroindenes were produced in good yield and with high stereoselectivity. Octahydronaphthalenes were also obtained, but the stereoselectivity was low and the IMDA reaction was more sensitive to steric hindrance.

A Facile Synthesis of Homofarnesene Components of Fire-Ant Trail Pheromone

SHANG-SHING P. CHOU (周善行) AND WU-HWEI LEE

Synthesis, 219-220 (1990)

An efficient four-step synthesis of the homofarnesene components of fire ant trail pheromone starting with geranyl bromide and 2, 3-dimethyl-4-phenylthio-2, 5-dihydrothiophene-1, 1-dioxide has been accomplished.

Mixed Sulphur and Phosphorus Ylide Complexes of Palladium formed by Phasetransfer Catalysis, X-ray Crystal Structure of $[Pd\{(CH_2)_2S(O)Me\}\{Ph_2PCH_2PPh_2CH(O)Ph\}]I\cdot CH_2Cl_2\cdot H_2O$

IVAN J. B. LIN (林志彪), H. C. SHY AND C. W. LIU

J. Chem. Soc. Dalton Trans., 2509 (1990)

Phosphorus ylide complexes $[PdBr_2\{Ph_2P(CH_2)_nPPh_2CHC(O)R\}]$ (n=1 or 2; R=Me, Ph, or OEt), and mixed sulphur and phosphorus ylide complexes $[Pd\{(CH_2)_2S(O)Me\}\{Ph_2P(CH_2)_nPPh_2CHC(O)R\}]I$, have been synthesized by the phase-transfer technique. The presence of the phase-transfer catalyst has only a marginal effect in the preparation of phosphorus ylide-containing complexes. The mixed ylide compounds have both a chelated double sulphur ylide and a C, P-chelated phosphorus ylide. A mixed-ylide complex $[Pd\{(CH_2)_2S(O)Me\}\{Ph_2PCH_2PPh_2CHC(O)Ph\}]I\cdot CH_2Cl_2\cdot H_2O$ has been investigated by means of X-ray crystallography. The Pd-C bond length of 2.183(5) Å for the phosphorus ylide co-ordination is longer than that for the sulphur ylide co-ordination [2.094(3) Å average].

Phase-Transfer-Catalyzed P-C Bond Cleavage in Platinum Bis(diphenylphosphino)methane Complexes under Exceedingly Mild Conditions

IVAN J. B. LIN (林志彪), J. S. LAI AND C. W. LIU

Organometallics, **9**, 530-531 (1990)

The reaction of $[Pt(dppm)Cl_2]$ (dppm=$Ph_2PCH_2PPh_2$) with $[S(O)Me_3]Cl$ under basic phase-transfer-catalyzed conditions gave the complex $\{Pt(PPh_2Me)[PPh_2(OH)][(CH_2)_2S)O)Me]\}Cl$, which contains a bidentate sulfur ylide and two monodentate phosphine ligands. The latter was produced by the facile base hydrolysis of the dppm ligand, a reaction that is general for other Pt-dppm complexes.

Preparation of Sulfur Ylide Complexes of Palladium by Phase-Transfer Catalysis

REY F. WU, IVAN J. B. LIN (林志彪), G. H. LEE, M. C. CHENG AND YU WANG

Organometallics, **9**, 126-130 (1990)

Sulfur ylide complexes of palladium were prepared under basic phase-transfer catalysis. Increasing the amount of phase-transfer catalyst enhanced the rates of formation of the complexes. The optimal range of base concentration was found to be 1.0-2.0 N. The proposed role of the phase-transfer catalyst is to carry OH^- into the organic layer and to prevent the ylide from abstracting a proton from water present in the organic phase. The single-crystal structures of $\{Pd(PPh_3)_2[(CH_2)_2S(O)(CH_3)]\}I$ and $Pd(PPh_3)(I)[(CH_2)_2S(O)(CH_3)]$ were determined. The former crystallized in the monoclinic space group $P2_1/n$, with a=11.337(2) Å, b=21.954(3) Å, c=15.406(2) Å, β=94.30(1)°, V=3,823.6 Å^3, Z=4, and R=0.095 for 4,906 observed reflections. The latter crystallized in the orthorhombic space group $P2_12_12_1$, with a=9.691(3) Å, b=14.579(2) Å, c=15.642(3) Å, V=2,209.9 Å^3, Z=4, and R=0.078 for 2,201 observed reflections. Both compounds have rather short ylidic S-C bond (1.60-1.70 Å).

The Molecular Structure of a Novel Diplatinum Compound $H[(Et_2N{=}CS_2)Pt(PPh_2Me)(PPh_2O)]_2^+PF_6^-$ Obtained from Phase-Transfer Base Hydrolysis of $[(Et_2N{=}CS_2)Pt(PPh_2CH_2PPh_2)]Cl$

LING-KANG LIU, YUH-SHENG WEN, IVAN J. B, LIN (林志彪), J. S. LIA AND C. W. LIU

Bull. Inst. Chem., Academia Sinica, **37**, 65-73 (1990)

Base hydrolysis of $[(Et_2N{=}CS_2)Pt(PPh_2CH_2PPh_2)]Cl$ under phase transfer catalytic conditions, followed by an anion exchange with NH_4PF_6 has produced in 80% yield a novel diplatinum compound $H[(Et_2N{=}CS_2)Pt(PPh_2Me)(PPh_2O)]_2^+PF_6^-$. An x-ray structure analysis has resulted in an orthorhombic space group Pccn with cell dimensions a= 27.380(11), b=13.604(2), c=17.569(4) Å, V=6,544(3) Å^3, Mr=1,635.48, Z=4, F(000)=3,223.35, Dc=1.660 g/cm^3, μ=4.62 mm^{-1} for Mo-Kα radiation, and R=0.030 for 3,354 reflections with Io$\geq 2\sigma_I$. The structure of this compound consists of discrete PF_6^- anions and very large cations formed by a proton bridged binuclear species, $H[Et_2N{=}(CS_2)Pt(PPh_2Me)(PPh_2O)]_2^+$.

Preparation of Sulfur Ylide Complexes of Platinum by Phase Transfer Catalysis

J. S. LIA, REY F. WU AND IVAN J. B. LIN (林志彪)

Various sulfur ylide complexes of platinum have been prepared by the phase transfer catalysis (PTC). Thus, reaction of $Pt(PR_3)_2Cl_2$ (R=methyl or phenyl) in CH_2Cl_2 with $[S(O)(CH_3)_3]I$ under PTC/OH^- conditions, give complexes $\{Pt(PR_3)_2[(CH_2)_2S(O)(CH_3)]\}I$, which contain a bidentate double sulfur ylide. With $Pt(dppe)Cl_2$ (dppe=$Ph_2P(CH_2)_2PPh_2$) as starting material, a similar product was obtained. But when $Pt(dppm)Cl_2$ (dppm=$Ph_2PCH_2PPh_2$) was treated with $[S(O)(CH_3)_3]Cl$ under PTC/OH^- conditions, an unexpected product $\{Pt(PPh_2CH_3)(PPh_2OH)$-$[(CH_2)_2S(O)(CH_3)]\}Cl$ was obtained. This compound contains a bidentate

double sulfur ylide and two unsymmetrical phosphines resulting from the base hydrolysis of dppm. Compoend $\{Pt(PPh_3)_2[(CH_2)_2S(O)(CH_3)]\}I$, was subjected to an X-ray diffraction study. The compound crystallized in the orthorhombic space group $Pna2_1$ with cell parameters $a=19.332(4)$, $b=11.101(5)$ and $c=16.936(5)$ Å, $Z=4$.

Involvement of *E. coli dcm* Methylase in Tn3 Transposition

MEI-KWEI YANG (楊美桂), SHIAO-CHING SER AND CHAO-HUNG LEE

Proc. Natl. Sci. Counc. B. R.O.C., **13**(4), 276-283 (1989)

The effect of DNA methyltransferases on Tn3 transposition were investigated. The *E. coli dam* (deoxyadenosine methylase) gene was found to have no effect on Tn3 transposition. In contrast, Tn3 was found to transpose more frequently in dcm^+ (deoxycytosine methylase) cells than in dcm^- mutants. When the *EcoR*II methylase gene was introduced into dcm^- cells (*E. coli* strain GM208), the frequency of Tn3 transposition in GM208 was dramatically increased. The *EcoR*II methylase recognizes and methylates the same sequence as does the *dcm* methylase. These results suggest that deoxycytosine methylase modified DNA may be a preferred target for Tn3 transposition. Experiments were also performed to determine whether the Tn3 transposase was involved in DNA modification. Plasmid DNA isolated from dcm^- *E. coli* containing the Tn3 transposase gene was susceptible to *Apyl* digestion but resistant to *Eco*RI digestion, suggesting that Tn3 transposase modified the *dcm* recognition sequence. In addition, restriction enzymes *Taq*I, *Ava*II, *Bgl*I and *Hpa*II did not digest this DNA completely, suggesting that the recognition sequences of *Taq*I, *Ava*II, *Bgl*I and *Hpa*II were modified by Tn3 transposase to a certain degree. The type(s), the extent and mechanism(s) of this modification remain to be investigated.

The Effect of Temperature and Moisture Content on Viability, Cell Division and Chromosomal Aberration of Tomato Seed

BAO-WEI LIU (劉寶瑋), SIAO-ZE YOUNG AND CHING-LONG LAN

生物科學 第三十二卷 第二期 第41-52頁 (1989)

Tomato (*Lycopersion esculentum* Mill.) seeds were treated with nine combinations of temperature (25°, 33°, and 40°C) and seed moisture content (8, 16, and 32%) for 120 days of storage. High moisture content was the predominant factor to cause the loss of seed germinability, and high temperature accelerated the aging process. The decrease of seed viability was closely associated with an increase in chromosomal aberrations and the reduction in ability of cell to divide in root meristems. The first mitotic division was also delayed to occur in the longer root length when the seed germinability was significantly decreased. The distribution of aberrant chromosome in various root lengths reached to the peak in the intermediate root lengths of aged seeds and then declined in the longest group of lengths of roots.

Polyribosome Changes of Germinating Rice Seeds After ^{60}Co Gamma-Irradiation

WOAN-FANG TZENG (曾婉芳) AND TI-SHENG LU

Journal of the Chinese Biochemical Society, 18(1), 29-37 (1989)

Scutellular tissues were dissected from germinating rice seeds irradiated with Co-60 *r*-ray. The incorporation of ^{3}H-leucine was examined by both *in vivo* and *in vitro* assay systems. It was found that at low doses, 5 and 20 Krad, the protein synthesis was not affected by the radiation in both assay systems. However, at high doses, 55 and 125 Krad, the incorporation of ^{3}H-leucine into protein was found 79 and 71% with respect to the control for *in vivo* assay. *In vitro* system they were 73 and 66% incorporation as compared with the control.

Rice seeds treated with gibberellin (20 ppm, 16 hr) before germination did not reduce the inhibiting effect on protein synthesis by radiation treatment in both assay systems.

The activities of both ribosomes and post-ribosome supernatant for protein synthesis were found to be inhibited by γ-irradiation at both 55 and 125 Krad. The inhibitory effect of ribosomes was more than that of post-ribosome supernatant. Polyribosome content was reduced at either 55 or 125 Krad. The reduction of polyribosomes could be one of the major factors resulting in the inhibition of protein synthesis.

幼 兒 發 展 與 評 量

林 惠 雅

幼兒教育年刊 第三期 第8-29頁 (1989)

幼兒發展與評量不論在幼兒教育或輔導上均扮演十分種要的角色。然而幼兒評量的意義和方式卻常被誤解。本文首先闡釋與討論幼兒評量的意義和方式，其次說明幼兒身心各方面的發展，以及幼兒發展與評量的關係。藉此使幼兒發展與評量的概念得以澄清，並且提供作爲設計幼兒評量之參考。

二位學前障礙幼兒與一般正常幼兒混合就讀之效果探討

蘇 雪 玉

蔡軒圖書出版社 (1990)

本研究係針對學前障礙幼兒與一般正常幼兒混合就讀的評估、輔導與追踪報告。

爲了找出安置學前障礙幼兒與一般正常幼兒混合就讀篩檢時的依據及指引以及探討學前混合就讀對輕度障礙幼兒是否可行和有效益，一位輕度障礙幼兒與一位中度障礙幼兒被安置在正常學前教育機構。經歷三年半，屬中度障礙幼兒，第一年實行混合就讀，後因干擾性行爲而轉介到特教機構，至第三年起又部分時間回歸普通班就讀。另一位輕度障礙幼兒則全程混合就讀並接受課外輔導，前三年在學前教育機構後半年在國小普通班。

本文研究的工具主要使用觀察與評量兩種方式：時間與事件抽樣觀察方法；評量則採用測驗和量表。

從以上的安排與測試，獲致的結果顯示輕度障礙幼兒的發展，由輕度、低常到中等有顯著的進步；而中度障礙幼兒雖在各方面均有進步和突破，但仍屬中度障礙程度。因此獲得的結論是，學前混合就讀計劃對輕度障礙幼兒是可行的，甚至學前混合就讀對小學低年級學習也有正面的效益。

最後本報告提供二項建議：其一，混合就讀篩選時必需考慮三項決定性因素：輕度障礙、不具干擾性行爲、行政主管及教師接納的態度。其二，提供一個簡易可行的學前混合就讀模式作爲混合就讀時的參考。

不同品系稻米及製程對發糕品質之影響

黃瑞美　林子清　蔣見美　呂政義

中國農業化學會誌　第二十八卷　第三期　第 267-275 頁　(1990)

本研究主要探討不同品系稻米及製作條件對傳統發糕品質之影響。以省產之臺中秈 10 號、臺中秈 17 號、臺中在來 1 號三種秈米與粳米之臺農 67 號共四種作材料來製作發糕，經外觀、體積、疏鬆度、質地粗細、顆粒大小及粘彈性等官能品評與物性測定，分別探討不同品系稻米之理化特性對發糕品質的影響，並分析發糕製作過程之影響因素，如磨粉與攪拌方法、米漿或米糊之置放時間與溫度對產品品質的影響。

實驗結果顯示，製程中如以濕磨製米漿，並經二段式高速攪拌手續，可改善發糕品質；米品種本身之理化特性影響發糕品質至巨，以高直鏈澱粉含量、硬凝膠與粘度回升值較大的不粘性米，如臺中秈 17 號與臺中在來 1 號，所製發糕體積大、組織疏鬆，呈沙質口感且老化極快；然低直鏈澱粉含量、軟凝膠及粘度回升值較小的粘性米，如臺中秈 10 號與臺農 67 號，所製發糕則體積小、組織緊密呈粘質口感且老化慢。

不同包裝方法對中式香腸貯藏品質之影響 II: 油脂及官能性質的變化

蔣見美　游淑媛　黃菜鳳

食品科學　第十七卷　第一期　第 23-36 頁　(1990)

用不同透氣率的包裝材料 PET/Al. foil/CCP、PVC/CPP、PP 和 NY/PE，施以充氮包裝及眞空包裝中式香腸後，分別置於 5°C，50% RH 和 12°C，50% RH 的貯藏環境中，定期就包裝袋內香腸之油脂酸價、過氧化價、脂肪酸

組成定量分析、TBA 值及品評分析包括定量描述分析和喜好程度品評分析等逐一檢查比較。

中式香腸應儘量置於低溫貯藏，貯藏在 12°C 的 PP 組因爲溫度高配合材料膜透氧率高，其油脂及官能評估品質變壞的速率最快。眞空包裝或充氮包裝中式香腸對油脂氧化速率並無顯著差異。五種不同方法所處理之中式香腸其多元不飽和脂肪酸酸變化並不顯著。隨著貯藏時間，香腸高品質的風味逐漸減低，尤其以 PP 組變化最大，5°C 組的變化最小。酸價高於 7 mg/g，TBA 值高於 2 mg/kg 是香腸敗壞不可食用時之臨界值。

不同包裝方法對中式香腸貯藏品質之影響 I: 微生物種類及菌數之變化

游淑媛 蔣見美 丘志威

食品科學 第十六卷 第四期 第 394-407 頁 (1989)

用不同透氣率的包裝材料 PET/Al. foil/CPP、PVC/CPP、PP 和 NY/PE，施以充氮包裝及眞空包裝中式香腸後，分別置於 5°C，50% RH 和 12°C，50% RH 的貯藏環境中，定期就包裝袋內氣體分析、水活性、總菌數、乳酸菌數、乳酸產量、pH 值、酵母及黴菌數和嗜冷性菌數等逐一檢查比較。

貯藏於 5°C 時對抑制香腸微生物效果最好。香腸採用眞空或充氮包裝對酵母及黴菌數有相同的抑制效果，然而眞空包裝對細菌生長的控制較充氮者佳。透氧性高的材質 PP 膜包裝的香腸，除了酵母及黴菌數，其他細菌數均較另外四種包裝顯著多，當貯藏於 12°C 達第三個月，其品質已不再被接受時的總菌數及嗜冷性菌數均高於 10^7/g，乳酸菌數高於 3×10^5/g，這些結果可當做香腸敗壞不可食用指標的參考。

金香葡萄的揮發性成分

黃淑雯 吳淳美 陳雪娥

中國農業化學會誌 第二十八卷 第二期 第 125-134 頁 (1990)

金香葡萄的揮發性成分經熱脫附／冷捕捉法 (TCT 法) 與吹除／注射法 (PTI 法) 收集，以氣相層析儀—質譜儀分析鑑定，共鑑定 78 種化合物，包括碳氫化合物 26 種、醇類 8 種、醛類 11 種、酮類 3 種、酯類 28 種和其他合物 2 種。以 PTI 法定量，發現 ethyl acetate、乙醇、丙酮含量最高，其次爲 ethyl butanoate、limonene 和 ethyl hexanoate。

Chromatographic Analyses of Xanthophylls in Egg Yolks from Laying Hens Fed Turf Bermudagrass (*Cynodon dactylon*) Meal

C. A. BAILEY AND B. H. CHEN (陳炳輝)

Journal of Food Science, **54**(3), 584-586 (1989)

The characterization of xanthophylls in egg yolks from laying hens fed turf bermudagrass (*Cynodon dactylon*) meal was studied. Laying hens were fed 2 wk on a milo-soybean meal diet to deplete the birds' xanthophyll stores from developing ova prior to introduction of 9% turf bermudagrass. After an additional 4 wk the various carotenoids present in egg yolks were determined by open-column, thin-layer, and high-performance liquid chromatography. Chromatographic analyses suggest that the yolk color was due mainly to the presence of free lutein and zeaxanthin at a ratio of 4:1. Neoxanthin and violaxanthin were present in minor amounts. The presence of β-carotene was not detected.

Effects of Dietary Fibers in Early Weaning on Later Response of Serum and Fecal Steroid Levels to High-Cholesterol Diet in Rats

YI-FA LU (盧義發), K. IMAIZUMI, M. SAKONO AND M. SUGANO

Nutrition Research, **9**, 345-352 (1989)

Male Wistar rats were early weaned at 16 days of age to a basal diet (BD) free of fiber or BD supplemented either with cellulose (CE), guar gum (GG), pectin (PE), polydextrose (PD) or cholestyramine (CY) for 2 weeks, then switched to a commercial rat ration for 4 weeks. Finally, a cholesterol-enriched diet was given to all rats for one week in order to study the imprinting effects of early dietary fiber consumption on cholesterol metabolism in later life. The water-soluble fibers (PE and PD) caused a lower level of serum cholesterol and apolipoprotein

(apo) E and a higher level of apo B. Apo A-IV levels decreased by supplementation of all the fibers tested. In later life early feeding of PE, PD or CY caused an increased level of serum cholesterol when challenged with a high cholesterol diet. A significant reduction of acidic steroid excretion in later time was observed only in rats fed CY in early life. The ratios of sterol-to-stanol and primary-to-secondary bile acids in feces tended to be lower in rats early fed water-soluble fibers. Thus, the present results strongly suggest that dietary fiber manipulation in early life exerts imprinting effects on steroid metabolism in later life.

Transient Control of Serum Cholesterol Homeostasis in Adult ExHC (Exogenous Hypercholesterolemic) Rats by Dietary Cholesterol during Weanling Period

YI-FA LU (盧義發), JUN MURAKAMI, AKIHIRO NAGATOMI, KATSUMI IMAIZUMI AND MICHIHIRO SUGANO

J. Nutr. Sci. Vitaminol., **35**, 463-474 (1989)

Rats hyper-responsive to a diet containing cholesterol plus cholic acid (exgenous hypercholesterolemic (ExHC) rats) were used to assess if cholesterol feeding at weanling period influences later serum cholesterol homeostasis. Diets containing cholesterol plus cholic acid (atherogenic diet) in early life, when compared to non-atherogenic diet, caused a transient suppression of serum cholesterol elevation in very-low- and low-density lipoprotein fractions during refeeding of the atherogenic diet in later life. Such an effect was not observed when ExHC rats were early given a diet supplemented with cholesterol or cholic acid alone, nor when ordinary Sprague-Dawley rats were given atherogenic diet. Early atherogenic diet caused an increased secretion of cholesterol as very-low-densit lipoprotein from the perfused livers of adult ExHC rats. Neither the activity of hepatic cholesterol-7α-hydroxylase of fecal steroid excretion in later life was influenced by the early dietary manipulation. Therefore, the present results show the deferred effect of early dietary manipulation on later serum cholesterol metabolism in ExHC rats, but the underlying mechanism(s) remains to be determined.

Effects of Cutting and Cooking Methods on the Shape Forming Properties of Cocktail Shrimp Made of Tiger Prawn

SHUN-YAO HSU, KING-PONG LIN
AND GUOO-SHYNG W. HSU (王果行)

Journal of the Fisheries Society of Taiwan, **16**(2), 145-152 (1989)

Tail-on, cooked, peeled and deveined tiger prawn has been a delicacy in restaurants and on cocktail tables. The shape and curvature of the shrimp could affect it's hanging stability on cocktail glasses. In this study, the effects of heating conditions and cutting methods on the curvature, shrinkage ratio, yield and textural properties of cocktail shrimps were investigated. The results indicated that cut position and cut length did not significantly ($p>0.05$) affect any of the measured quality attributes. Heating temperature, time and their interaction showed significant ($p<0.01$ or 0.05) effects on the yield, shrinkage ratio, curvature and texture of the final products and indicated the existence of an optimal heating condition. Shrinkage ratios R2, R3 and R31 appeared to be better parameters than other parameters which have also been tested in the study in searching for a indicator of hanging stability of the product.

探討葡萄單寧酸與蛋白質之作用模式

陳炯堂　何慧如　楊佩琪　李選能

食品科學　第十七卷　第二期　第105-113頁　(1990)

利用葡萄中單寧酸與多胜肽（多甘胺酸、多丙胺酸、多麩胺酸、多苯甲基麩胺酸、多脯胺酸）交互作用之研究可探討單寧酸與蛋白質之主要鍵結之形式及強度。分析時，分別將單寧酸、多胜肽溶於 phenylhydrazine 及 Trifluoroacetic acid (4:1，v/v) 之溶液中。由微分掃瞄熱卡的分析結果顯示單寧酸與多胜肽之作用焓差依序爲：多麩胺酸、多甘胺酸＜多丙胺酸、多苯甲基麩胺酸＜多脯胺酸。由此可知單寧酸與蛋白質較可能的交互作用是嫌水鍵之結合，而非離子鍵或氫鍵。

爲了瞭解及模擬單寧酸在食品中與蛋白質之作用力，必需探討兩者在水溶液中之作用力情形。由於多胜肽水溶性低，利用羧甲基化纖維素固定多胜肽，以提高水溶解度。初步實驗是採用多丙胺酸與羧甲基纖維，經化學耦合反應生成，產率是每公克乾重耦合物含 18.5 mg 多丙胺酸。此亦證實耦合反應之可行性。由微分掃瞄熱卡的分析結果顯示，單寧酸與耦合物作用之焓差比未耦合之多丙胺酸大。

Stability of Fish Oil in a Purified Diet with Added Antioxidants: Effects of Temperature and Light

CHINGMIN E. TSAI (蔡敬民), JOSEPH T. WOOTEN AND DAVID A. OTTO

Nutrition Research, **9**, 673-678 (1989)

The extent of oxidation of fish oil with added antioxidants in a purified diet was studied after storage under nitrogen at 1° or −16°C, and after exposure to air at room temperature with direct or indirect light. The thiobarbituric acid values showed that the fish oil diet was stable for at least two weeks when stored in the dark at 1° or −16°C. The fish oil diet was rapidly oxidized at room temperature when the diet was directly exposed to overhead fluorescent light. However, if the diet was exposed to only indirect light it was stable at room temperature for at least 8 days. These data emphasize the importance of light exposure when considering the stability of fish oil containing diets even in the presence of antioxidants. The data demonstrate that when feeding animals, daily mixing and replacement of fish oil containing diets (with added antioxidants) is not necessary if the diet is shielded from direct light.

不同飽和度食用油脂對脂質代謝之影響：P/S 非爲脂質代謝之良好指標

賈宜琛　林子清　吳金蒔　蔡敬民

中華民國營養學會雜誌　第 15 卷　第 1-2 期　第 25-39 頁　(1990)

本實驗的目的在探討不同食用油脂，以及食用時間長短對大白鼠脂質代謝的

影響。根據飽和脂肪酸、單元不飽和脂肪酸、多元不飽和脂肪酸的含量選出六種實驗油脂—黃豆沙拉油、液態豬油、花生油、米糠油、麻油、魚油；並將 108 隻成熟雄性 Sprague-Dawley 大白鼠分成六組，每組分別餵飼添加 13% 不同油脂的飼料，於 2、4、8 星期觀察脂質的變化；並測定血漿總脂質、三酸甘油脂、膽固醇、血漿低密度脂蛋白膽固醇 (LDL-C) 和高密度脂蛋白膽固醇 (HDL-C)、紅血球脆度、肝臟 Glucose-6-phosphate dehydrogenase (G6P-DH) 的活性。結果顯示魚油組之血漿總脂質、三醉甘油脂、膽固醇和肝臟 G6P-DH 的活性在各組中最低，也最易溶血 ($P<0.05$)。另液態豬油的脂肪酸飽和度最高，P/S 值最低，但液態豬油組的血漿總脂質、三酸甘油脂、膽固醇並未高於魚油之外的其他各組，其血漿總脂質和膽固醇甚至低於米糠油組 (8 週時)。另外米糠油組和花生組的肝臟 G6P-DH 活性與血漿三酸甘油酯值也明顯高於其他組 ($P<0.05$)。結果也顯示飼養 8 週時，各組間血脂質值比 2 和 4 週較可看出有明顯的差異存在。

The Biblical Version of the Origin and Significance of Clothing Based on Genesis

MARYTA M. LAUMANN (羅麥瑞)

Journal of the International Association of Costume, **6**, 145-151 (1989)

Clothes are a uniquely human invention. The debate on the original function of clothing and the significance of various proposed theories by anthropologists psychologists, moralists and other clothing experts is an ongoing one. The so-called modesty theory is considered among the major theories. Textbooks and reference books not seldom refer to the Genesis of the Christian Bible in defense of modesty.

This research investigates the true nature of human modesty. It not only rejects the use of Genesis in defense of the modesty theory as superficial and misleading but, moreover, reveals the real meaning and significance of the nakedness/clothing symbolism in the biblical book of origins. Based on insights that derive from a more comprehensive study of related texts of the Old as well as New Testament, it resolves apparent contradictions and discrepancies through the discovery of the double character of the clothing/nakedness symbolism used in Genesis and consistantly employed throughout the Scriptures as a whole.

Pipelined Microcomputers for Digital Signal and Image Processing

BRIAN K. LIEN (連國珍) AND GREGORY Y. TANG

Optical Engineering, 28(9), 943-948 (1989)

A multiple microcomputer system for digital signal and image processing applications is presented. A simple ring structure is employed to organize the multiple microcomputers. The data flow in the ring structure is is unidirectional. A task can be partitioned and distributed among the microcomputers, making possible pipelined execution of a task. Implementation with the use of the TMS32010 signal processing CPU and IBM PC is demonstrated. A design to ensure the program synchronization is also shown. Algorithms for carrying out infinite impulse response filtering, the fast Fourier transform, and the McClellan transform method of 2-D finite impulse response filters are developed. Experimental results are presented.